RI 8547

Bureau of Mines Report of Investigations/1981

A Mixed Kinetics Dump Leaching Model for Ores Containing a Variety of Copper Sulfide Minerals

By B. W. Madsen and M. E. Wadsworth

UNITED STATES DEPARTMENT OF THE INTERIOR

Report of Investigations 8547

A Mixed Kinetics Dump Leaching Model for Ores Containing a Variety of Copper Sulfide Minerals

By B. W. Madsen and M. E. Wadsworth

UNITED STATES DEPARTMENT OF THE INTERIOR
James G. Watt, Secretary
BUREAU OF MINES

This publication has been cataloged as follows:

Madsen, Brent W

A mixed kinetics dump leaching model for ores containing a variety of copper sulfide minerals.

(Report of investigations ; 8547)

Bibliography: p. 26-27.

Supt. of Docs. no.: I 28:23:8547.

1. Copper–Metallurgy–Mathematical models. 2. Leaching–Mathematical models. 3. Sulphides. I. Wadsworth, Milton E., joint author. II. Title. III. Series: United States. Bureau of Mines. Report of investigations ; 8547.

TN23.U43 [TN780] 622s [669'.3] 80-606872 AACR1

CONTENTS

ILLUSTRATIONS

ILLUSTRATIONS--Continued

TABLES

A MIXED KINETICS DUMP LEACHING MODEL FOR ORES CONTAINING A VARIETY OF COPPER SULFIDE MINERALS

by

B. W. Madsen [1] and M. E. Wadsworth [2]

ABSTRACT

To help maintain an adequate supply of minerals to meet national economic and strategic needs, the Bureau of Mines developed a mathematical model that describes acidic ferric sulfate leaching of copper from sulfide ores. The leaching model can aid in maximizing minerals and metals recovery from primary sources by giving operators and management a better understanding of the copper leaching process. This will aid in improving dump leaching operations. The model is based on a steady-state approximation of the continuity equation for diffusion of ferric ions in the rock pores and the intrinsic leaching kinetics of the various sulfide mineral particles. Ore characteristics included in the model were ore particle-size distribution, particle shape, grade, mineral content, mineral particle size, porosity, and tortuosity. The continuity equation was used with ferric ion concentration gradients and a fixed value for the diffusion coefficient. Except for effective diffusivity, each of these factors was either measured experimentally or estimated from theoretical considerations. The effective diffusivities were determined by fitting calculated leaching curves with experimental leaching data. Vertical variations in leach solution composition and temperature within a dump are not considered in this model. The model accurately predicted copper extractions for several large-scale tests during nearly 500 days of leaching.

INTRODUCTION

In the domestic mining of 260 million tons of copper ore in 1975, nearly 690 million tons of waste were moved and discarded (17).[3] This waste contained copper at a grade too low to permit profitable copper extraction using modern milling techniques. Some of the waste is leached with acidic solutions that percolate through the dump and dissolve a portion of the copper. Dump leaching is an important supplement to open pit-mill production of copper,

[1]Metallurgist, Salt Lake City Research Center, Bureau of Mines, Salt Lake City, Utah (now with Albany Research Center, Bureau of Mines, Albany, Oreg.).
[2]Assistant Dean, College of Mines and Mineral Industries, University of Utah, Salt Lake City, Utah.
[3]Underlined numbers in parentheses refer to items in the list of references preceding the appendixes.

providing about 10 percent of the total copper recovered. Because dump leaching is slow and incomplete, much copper remains in the dumps after leaching has been terminated. Research to improve leaching efficiency is carried out by the Bureau of Mines as part of its mandate to assure adequate domestic supplies of essential metals.

Mechanisms of the dump leaching art are not well known, and a better understanding can improve the operation's effectiveness. The careful delineation of leaching mechanisms followed by mathematical incorporation in a quantitative model may assist in dump leaching optimization. This report describes the development by the Bureau of a dump leaching model for determining the response of copper sulfide minerals to many of the conditions in large dumps leached with acidic ferric sulfate solution. The model can provide an upper limit for copper extraction from a dump containing copper as sulfide minerals. Hopefully, application of the model will be a step towards achieving more rapid, more complete, and less expensive recovery of copper from leach dumps.

Because of the increasing importance of dump leaching for augmenting copper production, more investigators are attempting to unravel the complex mechanisms involved. Results of these investigations are being presented as mathematical models. For example, a shrinking core model was used by Madsen (11), Braun (4), and Roman (16) to describe copper leaching. This model considered a core of unreacted ore that was separated from a reacted crust by an inward-moving reaction zone. The leaching kinetics involved a steady-state diffusion of reactants through the reacted portion of the ore fragment followed by a chemical reaction at the fresh surface of the mineral. When the chemical reactions were rapid compared with the diffusion rate of the reactants, the model, which assumed a constant-thickness reaction zone, satisfactorily described oxygen leaching of chalcopyritic ore at elevated temperatures and pressures, ferric sulfate leaching of chalcocitic ore at ordinary temperatures and pressures, and leaching of oxide copper ores. This model, however, cannot satisfactorily predict copper leaching when chemical reactions are slow relative to the diffusion rate of the oxidant in which the reaction zone thickens with leaching time. Thus, a different model must be used to describe the ferric sulfate leaching of copper at ordinary temperatures and pressures from ores containing refractory minerals such as chalcopyrite.

A more rigorous model using the continuity equation was devised by Bartlett for describing the copper leaching rate from low-grade chalcopyritic ore (1). This model involves the kinetics of chalcopyrite grains reacting with oxygen and diffusion of dissolved oxygen within the rock pores. The predicted copper extractions and Braun's experimental results differed (4). Later, the Bartlett model was modified and experimentally verified by Braithwaite (3) for the autoclave leaching of chalcopyrite ore particles with oxygen.

Both the reaction zone and the continuity models furnished a basis for this study, which extends the theory to incorporate intrinsic leaching characteristics of each of the contained sulfide minerals. The model described in this paper uses the continuity equation and includes kinetic expressions for sulfide minerals including chalcopyrite, chalcocite, covellite, and

pyrite. The model was derived after interpreting the results of large-scale, long-term laboratory leaching tests. Other leaching results were used to evaluate the accuracy of predicted copper extractions.

COPPER LEACHING FUNDAMENTALS

Copper extraction from waste dumps of low-grade sulfide ores using weakly acidic ferric sulfate solutions proceeds by a series of complicated, not well understood, mechanisms. The mechanics are complicated by the variety of minerals contained in the dump and the changing nature of the dump due to seasonal temperature variations, wet and dry periods, and variations in dump permeability with position and time. Generally, copper leaching requires a supply of both ferric ions to oxidize the sulfides and acid to dissolve copper oxides and to keep dissolved material in solution. Continued copper leaching at a reasonable rate requires ready access to oxygen and certain microorganisms that oxidize inactive ferrous ion to ferric ion, eliminating the need for continual addition of fresh ferric sulfate. Under favorable leaching conditions, the sulfide minerals react and form soluble cupric sulfate and ferrous sulfate and insoluble sulfur. Leaching ceases when the supply of ferric ions is depleted either through lack of leach liquor circulation or through conditions unfavorable for ferrous oxidation.

EXPERIMENTAL PROCEDURE

Laboratory leach testing was done on a large scale [~6,000 kg (13,227 pounds)] to provide data for samples containing larger fragments than could be leached in bench-scale apparatus. Tests were also conducted using a smaller sample [~200 kg (400 pounds)] for scaleup modeling studies. The large-scale tests were of sufficient size and more readily amenable to scaling up to a commercial venture than bench-scale tests. Leaching results were used to aid in model development and to check the model's predictions of leaching rates.

Five different copper sulfide samples were leached in the experimental equipment. Ore size distributions, weights, copper analyses, and mineral contents are shown in table 1. The first sample was a monzonite ore containing chalcocite (Cu_2S) as the most abundant copper mineral with minor amounts of chalcopyrite ($CuFeS_2$). The second sample was a quartz monzonite ore containing covellite (CuS), bornite (Cu_5FeS_4), chalcopyrite, and chalcocite. The third sample was also a quartz monzonite ore from the same mine as the second sample and contained the same mineral types. These two samples will be referred to as quartz monzonite I and quartz monzonite II in order to differentiate between them. The fourth sample was a granitic ore containing copper only as chalcopyrite. The fifth sample was a metasediment ore containing chalcocite, native copper (Cu), and trace amounts of cuprite (Cu_2O). The weight-percent pyrite for the five samples was 2.7, 6.9, 4.8, 2.9, and 1.2 for the monzonite, quartz monzonite I, quartz monzonite II, granitic, and metasediment samples, respectively. Since the leaching rate of the individual mineral particles is a function of their original size, mineral particle sizes were determined microscopically, and an average size was used for each mineral type in each ore sample. The large ore samples were leached in fiberglass

columns 1.37 meters (4.5 feet) in diameter by 3.04 meters (10 feet) high, and the loading capacity was about 8,000 kg (17,637 pounds). In case of the smaller [~200-kg (440-pound)] samples, the ore was leached in 189-liter (50-gallon) stainless steel drums. Solution was evenly distributed over the top of each column by a perforated rotating arm. Figure 1 shows two of the leaching columns.

TABLE 1. - Head analysis of samples leached

Ore	Size distribution	Weight, pounds	Copper grade, percent	Copper minerals, weight percent				
				Cu_2S	CuS	$CuFeS_2$	Cu_5FeS_4	Cu°
Monzonite...	Minus 6- plus 1/2-inch.	8,646	0.127	80	0	20	0	0
Do.....	Minus 13- plus 1/2-inch	9,736	.146	80	0	20	0	0
Quartz monzonite I.	Minus 6- plus 1/2-inch.	14,669	.200	60	16	20	4	0
Do.....	Minus 20-inch.....	17,456	.250	60	16	20	4	0
Quartz monzonite II.	Minus 15-inch.....	15,000	.227	66	17	14	3	0
Do.....	Minus 6- plus 1/2-inch.	458	.215	66	17	14	3	0
Granitic....	Minus 6- plus 7/8-inch.	12,998	.307	0	0	100	0	0
Metasediment	Minus 9- plus 1/2-inch.	11,741	.396	65	0	0	0	35
Do.....	Minus 2- plus 1/2-inch.	377	.430	65	0	0	0	35

The samples were leached by downward percolation of dilute ferric sulfate solutions at pH 2.0. Leach solution flow was 20.5 gallons per square foot per day, and solutions were recycled until the copper content was 1 to 2 grams per liter. Then circulation was discontinued, the column was allowed to drain, and the copper was recovered either by cementation on iron or by solvent extraction. After a drying or resting period of about 4 days, leaching was continued with effluent solutions from the copper recovery step. The nearly copper-free pH 2 solutions contained other metallic ions including iron, magnesium, aluminum, calcium, manganese, and zinc. Although natural buffering generally maintained the solution pH at nearly 2, sulfuric acid was added occasionally to prevent ferric iron from precipitating. These conditions typify an ideal portion of the leaching dump where good copper extraction can be achieved. The ionic strength of the leach solutions increased with recycling as other ore components in addition to iron and copper dissolved in the weak acid.

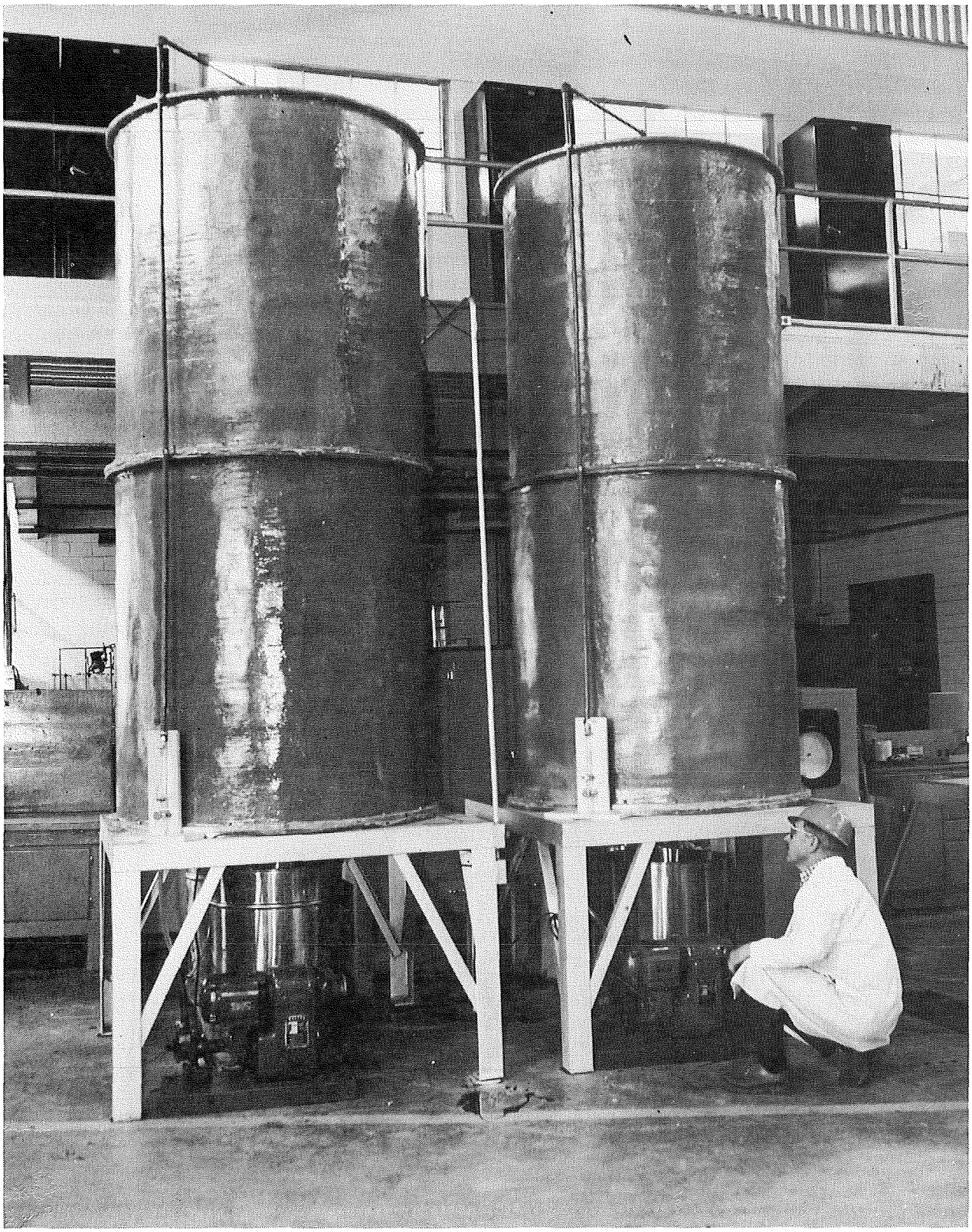

FIGURE 1. - Frontal view of leaching columns showing solution pumps and surge tanks.

MODEL DEVELOPMENT

Copper sulfide minerals dissolve when oxidized by ferric ions in acidic sulfate solutions. The reaction products include sulfate, elemental sulfur, and both ferrous and cupric ions. Copper dissolution rate primarily is a function of the ferric ion activity at the surface of the unreacted mineral grain. Ferric activity, as a function of position within the ore fragments, depends on the initial ferric ion concentration in the leach solution, ionic strength, temperature, solution chemistry, ferric diffusivity through channels in the porous ore particle, and ferric depletion resulting from reactions with either the copper mineral or with other ore constituents. Ferric depletion is controlled by the reaction kinetic characteristics of the reacting minerals. The hydrogen ion concentration must be maintained to provide favorable conditions for the autotrophic bacteria present, which actively oxidize ferrous iron to ferric maintaining effectively steady-state ferric concentrations in the bulk solution. Thus, many factors are involved in ore leaching, and no simple mathematical model neglecting intrinsic mineral kinetics can adequately describe the process. Attempts to use the mixed kinetic reaction zone model, previously used by Madsen (11) and Braun (4), failed to describe accurately the ferric sulfate leaching of ores containing a broad array of sulfide minerals.

A model based on the continuity equation for mass transfer was next applied. This model is more complex than the other models, and, because it cannot be solved analytically, numerical evaluation requiring high-speed computer equipment was used. In the model, intrinsic mineral reaction rates were included in a steady-state approximation of the continuity equation to determine the pore diffusion of ferric ions to the mineral surface, thus enabling copper extractions to be calculated. In the calculations, the authors assumed that the ore particles were surrounded by a uniform circulation of leach solution so that bulk solution transport was not a rate-controlling factor. The model did not include temperature effects, calculation of copper extractions from ores containing oxide copper minerals, or permeability of the ore bed. However, by use of the model one can predict an upper limit for copper extraction from a leach dump because the model describes leaching under ideal conditions of adequate air flow and constant temperature.

The Continuity Equation

Leach testing was done at room temperature, and temperature measurements made inside the column showed an essentially constant temperature. With a constant temperature and assuming the leach solution to be uniformly distributed around each ore particle, the modeling problem was reduced to solving the continuity equation for ferric ion distribution within the individual ore fragments.

The continuity equation for ferric ion distribution in an ore particle is[4]

$$\varepsilon \frac{\partial [Fe^{+3}]}{\partial t} = \Sigma R_k + D_{eff} \nabla^2 [Fe^{+3}]. \quad (1)$$

This expression is valid for ideal solutions where the activity coefficients of the diffusing species are equal to unity; that is, ionic activities equal ionic concentrations. However, according to Erdey-Grúz (7), chemical potential gradients and not concentration gradients should be used when describing diffusional processes. The solutes in a real mixture always diffuse from regions of higher activity towards those of lower activity. The activity effects were included in the effective diffusion coefficient. An empirical activity coefficient was used to relate the effective diffusion coefficient to the diffusion coefficient at infinite dilution according to the equation

$$D_{eff} = \gamma D_{eo}. \quad (2)$$

The ionic strength in solution-filled pores was assumed to be independent of ferric ion reduction to ferrous ion. Therefore, the activity coefficient was assumed to be constant throughout the solution-filled pore volume for a given point in time.

A pore theory proposed by Smith (18) states that the effective diffusion coefficient can be calculated by multiplying the ordinary diffusion coefficient by the porosity and dividing by the tortuosity. This is given by the expression

$$D_{eo} = \frac{\varepsilon D_o}{\tau}. \quad (3)$$

This equation allows values for the effective diffusivities to be calculated from physical parameters and ordinary diffusion coefficients. Unfortunately, values for the ordinary diffusion coefficients have not been tabulated for the variety of ferric ion complexes present, and tortuosities have not been determined experimentally. Comparison of model predictions with experimental results can be used for determining the effective diffusion coefficient at infinite dilution, D_{eo}.

The operator, ∇^2, depends on the geometry of the ore particles and is defined by the following equation for the case of spherical ore fragments, as given by

$$\nabla^2 = \frac{\partial^2}{\partial r^2} + \frac{2}{r} \frac{\partial}{\partial r}. \quad (4)$$

[4]Mathematical symbols used in the equations are defined in appendix A.

Spherical fragment geometry was used exclusively in this investigation. For spheres, equation 1 becomes

$$\varepsilon \frac{\partial c}{\partial t} = -\Sigma R_k + D_{eff} \left(\frac{\partial^2 c}{\partial r^2} + \frac{2}{r} \frac{\partial c}{\partial r} \right). \tag{5}$$

A steady-state approximation of the continuity equation can be applied if the consumption rate of ferric ions, ΣR_k, is much greater than the accumulation of ferric ions, $\varepsilon \frac{\partial c}{\partial t}$. Sohn and Szekely (19) used this approximation when interpreting data involving gaseous reaction in porous solids. The mathematical expression for the approximation is

$$\Sigma R_k >> \varepsilon \frac{\partial c}{\partial t} . \tag{6}$$

The assumption of steady state reduces the complex partial differential equation (equation 5) to a simpler ordinary differential expression of the continuity equation

$$\Sigma R_k = D_{eff} \left(\frac{d^2 c}{dr^2} + \frac{2}{r} \frac{dc}{dr} \right). \tag{7}$$

One way to solve the simplified continuity equation (equation 7) using high-speed computer techniques requires finite difference approximations for the derivatives. This was done by the mathematical leaching concept in which the spherical ore particle was divided into concentric shells with a thickness Δr as described by Braithwaite (3). There are N numbers of positions located at the shell interfaces. These positions are designated with a subscript j. Position 1 (j=1) corresponds to the center of the fragment, and position N (j=N) corresponds to the outer edge of the fragment.

The relationship of the ferric ion consumption rate in terms of the mineral leaching rates is given by

$$\underset{k}{\Sigma} R_{jk} = \underset{k}{\Sigma} \left[\frac{\sigma_k \rho G}{MW_{Cu}} \right] \left[\left(\frac{d\alpha}{dt} \right)_{jk} \right]. \tag{8}$$

The term $\underset{k}{\Sigma} R_{jk}$ is the rate of consumption of ferric ions at position j for all k minerals in the fragment. The term $\left(\frac{d\alpha}{dt} \right)_{jk}$ (the fractional dissolution rate of mineral k at position j) is a function of ferric ion activity.

Intrinsic Mineral Leaching Kinetics

Knowledge of the leaching kinetics of individual ferric-ion-consuming minerals is necessary to describe the rate term, $\underset{k}{\Sigma} R_{jk}$, in equation 8. Laboratory leaching studies have been conducted by a number of investigators with the data mathematically modeled, and the results were used in this study. The pertinent minerals include chalcocite, secondary covellite formed by the

reaction of ferric sulfate and chalcocite, natural covellite, chalcopyrite, and pyrite. Bornite and cuprite were excluded because of the small quantity of these minerals in the ores tested. Native copper leaches very slowly with acid ferric sulfate, therefore in the model calculations it was assumed to leach at the same rate as chalcopyrite.

Chalcocite

The dissolution of chalcocite (Cu_2S) with ferric sulfate occurs in two stages (12). The first stage is the conversion of chalcocite to secondary covellite ($Cu_{1.2}S$), according to the following chemical equation:

$$5Cu_2S + 8Fe^{+3} \rightarrow 5Cu_{1.2}S + 4Cu^{+2} + 8Fe^{+2}. \quad (9)$$

Marcantonio (12) described the leaching mechanisms as an electrochemical reaction and showed that at low temperatures the first stage was essentially complete before the second stage started. The leaching kinetics were controlled by the particle size, temperature, fraction of the first-stage leaching completed, and ferric ion activity. Deviations of apparent activities of the ferric ions and activities calculated from thermodynamic and theoretical considerations involving the extended Debye-Huckel theory (12) were accounted for by including a chemisorption term, which effectively reduced the apparent activity of the ferric ions. However, if an apparent activity coefficient is used in place of the chemisorption term in Marcantonio's model, the following expression describes the leaching kinetics of the first stage of chalcocite leaching:

$$\frac{d\alpha'}{dt} = \frac{k' (1-\alpha') \gamma[Fe^{+3}]}{r_o}. \quad (10)$$

The determination of values for the apparent activity coefficient, γ, is described later in this report.

Secondary Covellite

Marcantonio (12) also observed that after 40 percent of the copper had been leached, the second stage of chalcocite leaching began, which can be represented by the reaction

$$5Cu_{1.2}S + 12Fe^{+3} \rightarrow 6Cu^{+2} + 5S^{\circ} + 12Fe^{+2}. \quad (11)$$

The kinetics of this stage followed the relationship

$$\frac{d\alpha''}{dt} = k'' \{\gamma[Fe^{+3}]\}^{0.54} (1-\alpha'')^{0.5}. \quad (12)$$

This equation includes Marcantonio's chemisorption effect in the apparent activity coefficient for ferric ions, γ. The leaching rate for secondary covellite was independent of particle size because secondary covellite is very porous and the transport rate of ferric ions through the porous structure is rapid relative to the leaching rate.

Natural Covellite

Natural covellite is less porous than secondary covellite. Dutrizac and MacDonald (5) determined the leaching rate for polished disks of covellite; when converted to spherical geometry, their rate equation is

$$\frac{d\alpha}{dt} = (1-\alpha)^{2/3}\left[\frac{k^{III}}{r_o}\right]\left[\frac{Fe^{+3}}{5 \times 10^{-6}}\right] . \qquad (13)$$

Equation 13 is valid for ferric ion concentration less than 5×10^{-6} mole/cm^3, and the term $\frac{[Fe^{+3}]}{5 \times 10^{-6}}$ can be neglected at ferric concentration exceeding 5×10^{-6} mole/cm^3. This equation can be altered to include the activity coefficient, γ, but the value of the rate constant k^{III} would have to be changed to give the same rates of reaction.

Chalcopyrite

Chalcopyrite dissolves in acidic ferric sulfate solutions by the following equation:

$$CuFeS_2 + 4Fe^{+3} \rightarrow Cu^{+2} + 5Fe^{+2} + 2S^o. \qquad (14)$$

Jones and Peters (10) attributed rate control to a surface reaction, whereas others (2, 5) report the reaction rate is limited by transport of iron through a layer of elemental sulfur. Munoz (14) recently reported the opinion that the rate-limiting step is the transport of electrons through the layer of elemental sulfur. The opinion was supported by the independence of the reaction rate with respect to ferric, ferrous, and cupric concentrations plus a high activation energy of 20 kcal/mole (84 kJ/mole). The high activation energy closely agrees with the value calculated for electron transport through elemental sulfur.

The following theoretical rate expression describes electron transport through the reaction layer of elemental sulfur:

$$\frac{d\alpha}{dt} = \frac{k^{IV}(1-\alpha)^{1/3}}{2r_o^2[1-(1-\alpha)^{1/3}]} . \qquad (15)$$

The integrated form of equation 15 with the boundary condition that α=o when t=o is

$$1 - (2/3)\alpha - (1-\alpha)^{2/3} = \frac{k^{IV}t}{3r_o^2} . \qquad (16)$$

Rate data from the initial stage of the reaction, before formation of an appreciable layer of sulfur, showed an inverse first-order dependence on the initial particle diameter, a half-order dependence on ferric concentration,

and an activation energy of 8 kcal/mole (34 kJ/mole). The initial reaction was described by equation 17:

$$\frac{d\alpha}{dt} = \frac{k^V (1-\alpha)^{2/3} [Fe^{+3}]^{1/2}}{r_o} . \qquad (17)$$

Equation 17 was used in this report because the sulfur layer was negligible. Only a small fraction of the chalcopyrite was dissolved, and the presence of sulfur-oxidizing bacteria minimized formation of elemental sulfur. The constant k^V in equation 17 was determined by assuming that the leaching rate for chalcopyritic ore equaled the leaching rate of the mineral. This assumption appeared reasonable after 500 days of leaching where the ferric ion activity profiles through even the largest ore particles were computed to be flat. After prolonged leaching, all minerals in the ore particles were exposed to the same ferric ion concentration, and the fractional leaching rate for individual mineral particles equaled the leaching rate of the entire ore sample. The leaching rate of chalcopyrite was assumed to be independent of ferric ion concentrations above 1×10^{-5} mole/cm^3 as shown by Dutrizac (6).

Pyrite

An expression for the consumption rate of ferric ions by pyrite particles is

$$\frac{d [Fe^{+3}]}{dt} = \frac{1.17 \times 10^4 \, WS \, [Fe^{+3}] \exp (-20.5 \times 10^3/1.987T)}{V \, [Fe_{tot}] \, [H^+]^{0.44}} . \qquad (18)$$

The rate of consumption has the units of moles per cubic centimeter per second, as presented in equation 18. This equation is equivalent to the expression derived by Mathews and Robins (13), except that the units have been changed to be consistent with those used in this study. The combination of terms (WS/V) in equation 18 is the total surface area of pyrite particles per cubic centimeter of ore particle, and all concentrations are expressed as moles per cubic centimeter. This equation was used in the mathematical leaching model, and the pyrite surface area, S, was calculated by microscopically determining both the amount and particle size of the mineral. The hydrogen ion concentration was assumed to be constant throughout the ore particles because of the uniform distribution of acid-generating pyrite.

Comparison of the Leaching Rates of Copper Minerals

Calculated leaching rates are compared in figure 2 for chalcocite, covellite, secondary covellite, and chalcopyrite. The curves for chalcocite and covellite dissolution were determined using equations 10, 12, and 13 for a temperature of 25° C using a leach solution 0.005 molar in ferric sulfate. The leaching rates of covellite and secondary covellite are intermediate between reactive chalcocite and refractory chalcopyrite. Figure 2 also shows that the first-stage leaching of chalcocite is much faster than that of any of the other minerals. However, as the amount of cuprous copper in the solid diminishes, the rate of copper extraction falls to nearly zero, according to

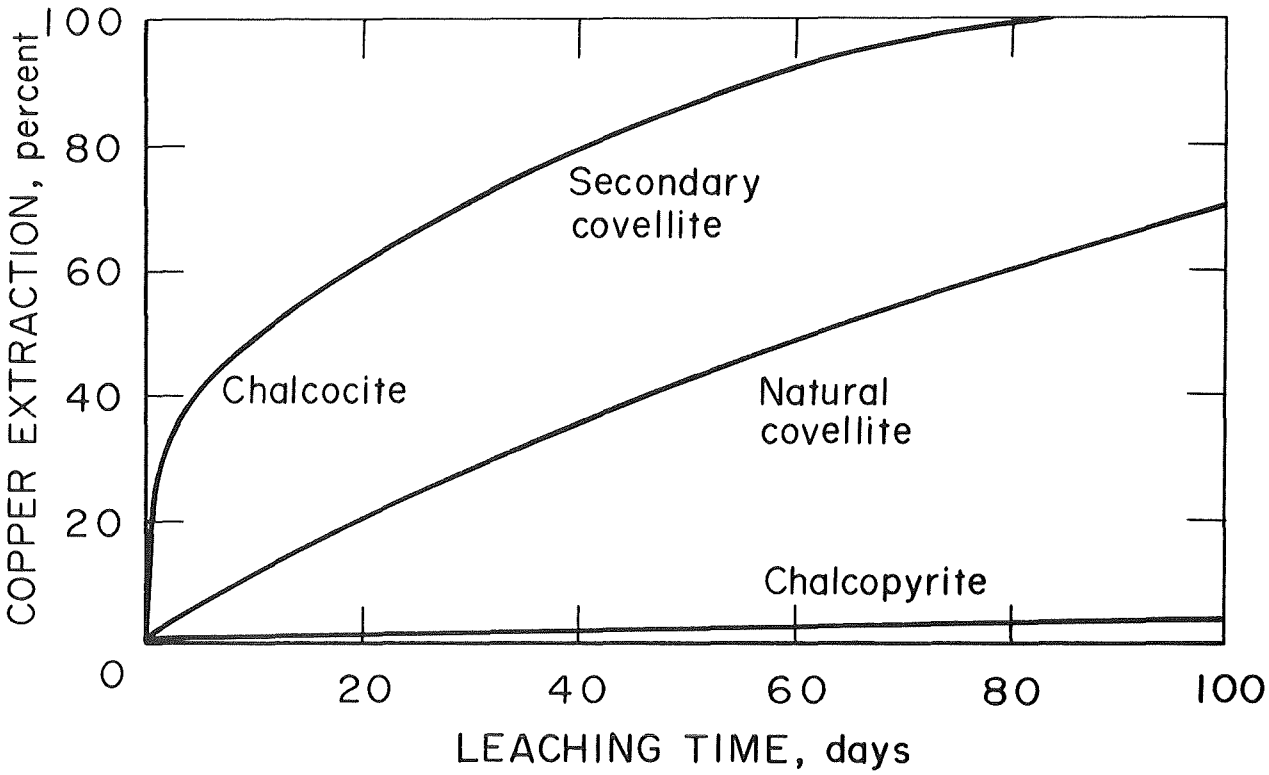

FIGURE 2. - Comparison of the calculated copper extractions for various pure minerals leached with 0.005 molar ferric sulfate.

equation 10. In fact, the mathematical expression never allows the fraction of copper reacted to exceed 0.40. An arbitrary value of 0.39 for the fraction reacted was used as a cutoff point where the first-stage leaching of chalcocite ends and the second-stage leaching commences. Natural covellite leaches somewhat slower than chalcocite or secondary covellite. Equation 13 was used to describe the leaching curve for the natural covellite. The slowest leaching mineral was chalcopyrite. Equation 17 was used to calculate the extraction curve for chalcopyrite. Thus, it might be expected that an ore containing an abundance of chalcocite will leach much faster than ore containing chalcopyrite as the main copper mineral.

Apparent Ferric Ion Activity

Ferric ion activity is an important factor in the rate equations. Mathematically predicted copper extractions were consistently higher than experimental extractions when ferric activity coefficients were derived from thermodynamic data and the Debye-Huckel theory. A similar disparity was noted by Marcantonio (12). The problem was resolved by using an apparent activity coefficient determined empirically by fitting equations 10 and 12 with Marcantonio's leaching data. The empirical expression for the apparent ferric ion activity coefficient is

$$\gamma = \exp\ (-1.373 - 239.7\ [Fe^{+3}]^{1/2} + 4870\ [Fe^{+3}]). \qquad (19)$$

Good agreement was achieved between calculated leaching rates, using the empirical activity coefficients, and experimental results. The ferric ion concentration for this comparison ranged from 0.01 to 1.0 molar. Confidence in the validity of equation 19 was reinforced by the similarity between calculated apparent ferric activities and measured activities for trivalent aluminum (8) and indium (9) in sulfate systems. The value for the activity coefficient as calculated in equation 19 was used in the kinetic leaching expressions (equations 10, 12, and 17) and also in the computation of the effective diffusion coefficient (equation 2).

Late Enhancement of the Leaching Rate

Results of copper ore leach testing showed that slightly enhanced leaching rates occurred during the later stages of the tests. This result led to including a factor in the model to describe the phenomenon. However, it must be emphasized that the inclusion of this factor in the model made only small adjustments in the predicted leaching curves. Braun (4) stated that late enhancement results from the generation of cracks and fissures, and the cracking of the leached particles was noted in this study. Braun proposed that a single parameter applied to both the chemically and diffusion controlled processes can be used to describe the late enhancement of the leaching rate. This parameter is a shape factor, ϕ_v, that varies systematically with the depth of a reaction zone and approaches some limiting degree of surface roughness. The shape factor was related to the fraction of copper leached as

$$\phi_v = [1 - (2/3)\lambda\alpha_v r_o^3]^{1/2}. \qquad (20)$$

In equation 20 the term λ is the late enhancement constant. As discussed later in this report, the late enhancement term and the effective diffusion coefficient are the only terms evaluated when fitting calculated curves to experimental leaching data. All other parameters were measured in the laboratory prior to leaching an ore sample.

A lower limit of 0.17 was placed on ϕ_v since smaller values would indicate undue fragmentation of the ore particle. The factor for late enhancement was entered in the leaching model by relating the term ε/τ in equation 3 to the shape factor as follows:

$$\varepsilon/\tau = \frac{(\varepsilon/\tau)_o}{\phi_v} . \qquad (21)$$

Particle-Size Distribution

The ore fragment sizes of the samples leached ranged from about 51 cm (20 inches) to minus 200 mesh. This range of sizes was not narrow enough to be adequately described by a single average particle size. Therefore, the model was extended to include the actual particle-size distribution and the grade of each size fraction.

A normal distribution of broken ore particles can be described by the Schuhmann relationship (20),

$$Y = \left(\frac{X}{K}\right)^Z , \tag{22}$$

where Y is the accumulative fraction passing size X (average diameter of an ore particle). A plot of log Y versus log X should result in a straight line with Z as the slope and K as the intercept. Figure 3 is presented as an example of such a plot and shows the particle-size distribution for the minus 33.02-cm (13-inch) plus 1.27-cm (1/2-inch) monzonite ore.

Using equation 22 and dividing the size distribution into L number of size intervals, a set of L+1 ordered pairs (X_I, Y_I) for X_I = K to X_I = Q can be calculated according to the equations

$$X_{I+1} = X_I P \tag{23}$$

and

$$Y_I = \frac{(X_I Z)}{K} . \tag{24}$$

This technique can be used if Q ≠ 0. If Q = 0, then an approximation can be made by setting Q at a positive value close to zero and allowing the

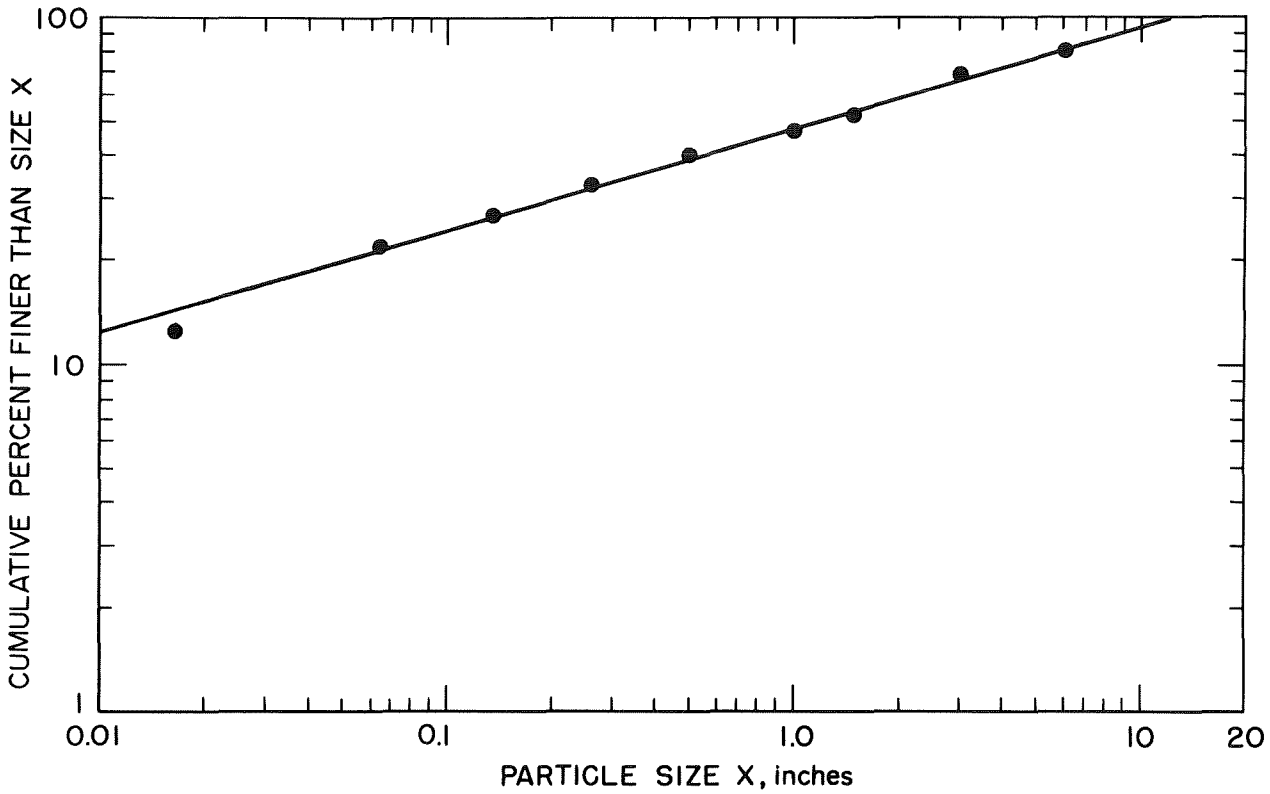

FIGURE 3. - Schuhmann plot of mine-run monzonite ore.

calculations to be carried out. The accumulative size distribution can then be separated into a set of L pairs (r_{io}, W_i) where W_i is the weight fraction of ore having an average radius r_{io} by the following relationships:

$$r_{io} = \frac{X_i + X_{i+1}}{4} \tag{25}$$

and

$$W_i = Y_{i+1} - Y_i. \tag{26}$$

The fraction of the copper reacted for the entire size distribution at time level ν is given by

$$\alpha_\nu = \sum_{i=1}^{L} \alpha_{\nu i} F_i. \tag{27}$$

Mathematical Leaching Model

All the factors discussed in the preceding text were included in a computer program consisting of a main program and three subroutines. Appendix B contains a description and the program listing for the leaching model. Also included in appendix B are the necessary instructions for feeding data into the computer. The computer language is Fortran V, and many of the computation techniques used were the same as given by Braithwaite (3).

Factors included in the leaching model were (1) maximum time and time increments, (2) effective diffusivity, (3) stoichiometry, (4) number of shells per particle, (5) intrinsic mineral leaching rate constants, (6) coefficients of polynominals to describe the ferric ion concentration in the bulk solution as a function of time, (7) molar ratio of pyrite to chalcopyrite, (8) late enhancement constant, (9) number of size intervals, (10) constants to calculate the particle size distribution, (11) mineralogy with respect to copper distribution, and (12) grade and density of the ore fragments. All these factors except the effective diffusivity and the late enhancement constant were determined prior to leaching an ore sample. These two factors were determined by correlating calculated copper extractions with experimental results.

Verification of the Leaching Model

The leaching model was evaluated for accuracy by comparing calculated copper extractions with experimentally determined values attained by leaching the monzonite and quartz monzonite I samples using acidic ferric sulfate. Two samples containing different size distributions were leached for each of these ore samples. The size range, weights, and other data concerning these tests are listed in table 1. In the process of determining the best values for the effective diffusivity, $D_{\varepsilon o}$, and the late enhancement term, λ, the model curve was fitted to the experimental data from the minus 15.24-cm (6-inch) plus 1.27-cm (1/2-inch) samples. The data and modeling results for these columns are included in figures 4 and 5.

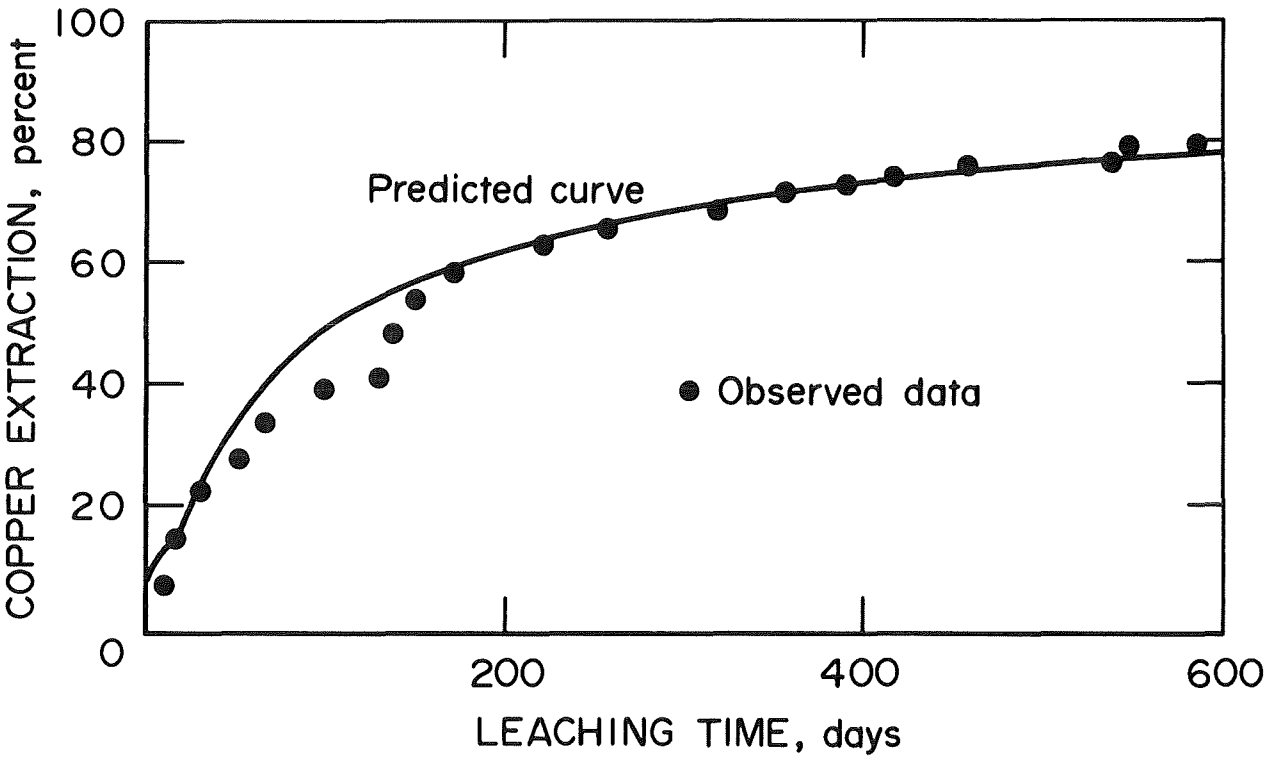

FIGURE 4. - Calculated copper extraction for monzonite ore [minus 15.24-cm (6-inch) plus 1.27-cm (1/2-inch)].

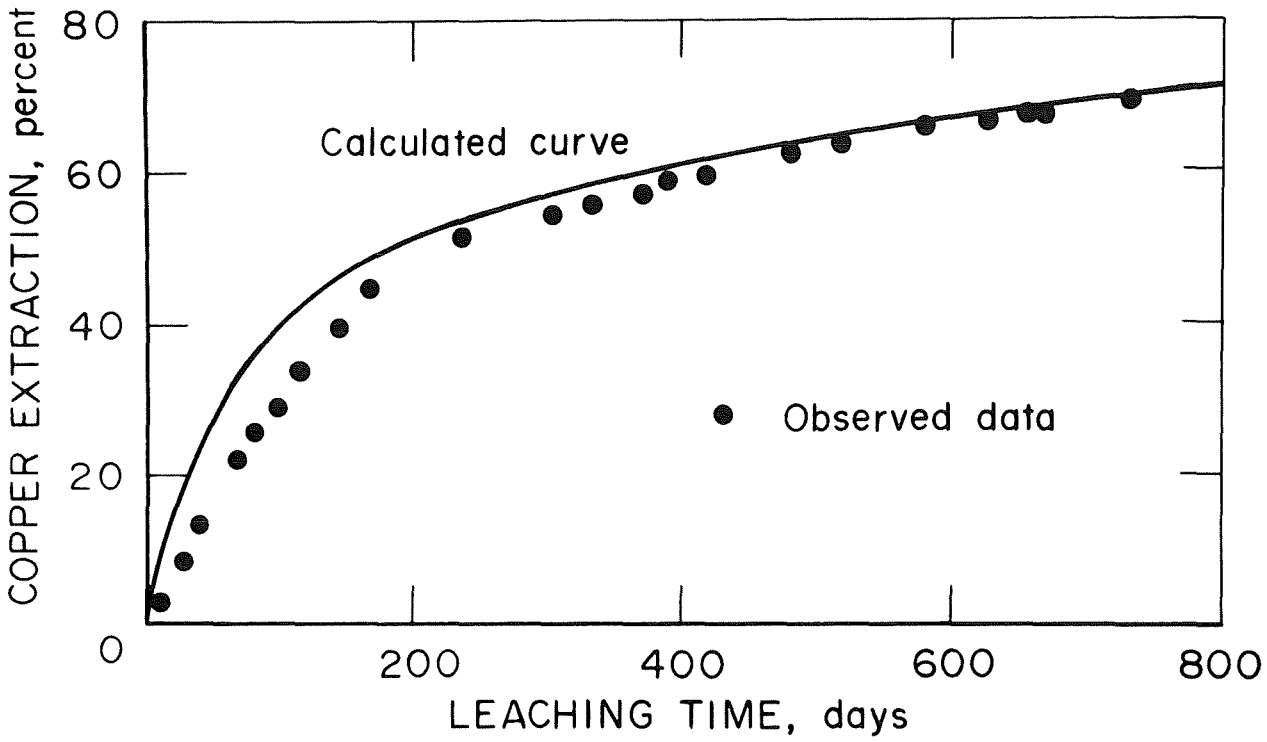

FIGURE 5. - Calculated copper extraction for quartz monzonite I ore [minus 15.24-cm (6-inch) plus 1.27-cm (1/2-inch)].

The unknown parameters for the granitic ore also were determined by fitting the calculated curve to the experimental data. Since the ore contained only chalcopyrite and since leaching is controlled by the mineral kinetics, the model was fitted by assuming that the effective diffusivity to be similar to that of the monzonite and quartz monzonite I ore (except for differences attributed to porosity differences). Figure 6 contains the calculated extraction along with experimental copper extractions for this ore.

Curve fitting to obtain leaching parameters is useful when the determined values are reasonable and can be successfully used to predict extractions for other experimental conditions. Testing the model's ability to accurately predict copper extractions for different ore size distributions was done using minus 33-cm (13-inch) plus 1.27-cm (1/2-inch) monzonite ore and minus 51-cm (20-inch) quartz monzonite I ore. The monzonite ore was screened to remove fine particles, but the quartz monzonite run-of-mine ore was not screened prior to leaching. Both predicted and experimental results are compared in figures 7 and 8. Predicted and experimental results were in good agreement for the monzonite ore; however, the predicted copper extraction for quartz monzonite I ore exceeded the experimental results. The disparity was caused by poor leaching conditions that developed early in leaching the run-of-mine quartz monzonite ore. Ore bed permeability became drastically diminished because salts precipitated in the ore fines, and portions of the ore were denied access to necessary ferric ions. Leach liquor circulation rate decreased from 835 l/m^2/day (20.6 gal/ft^2/day) to only 33 l/m^2/day (0.82 gal/ft^2/day) by the 461st day of leaching. Thus, good leach liquor circulation

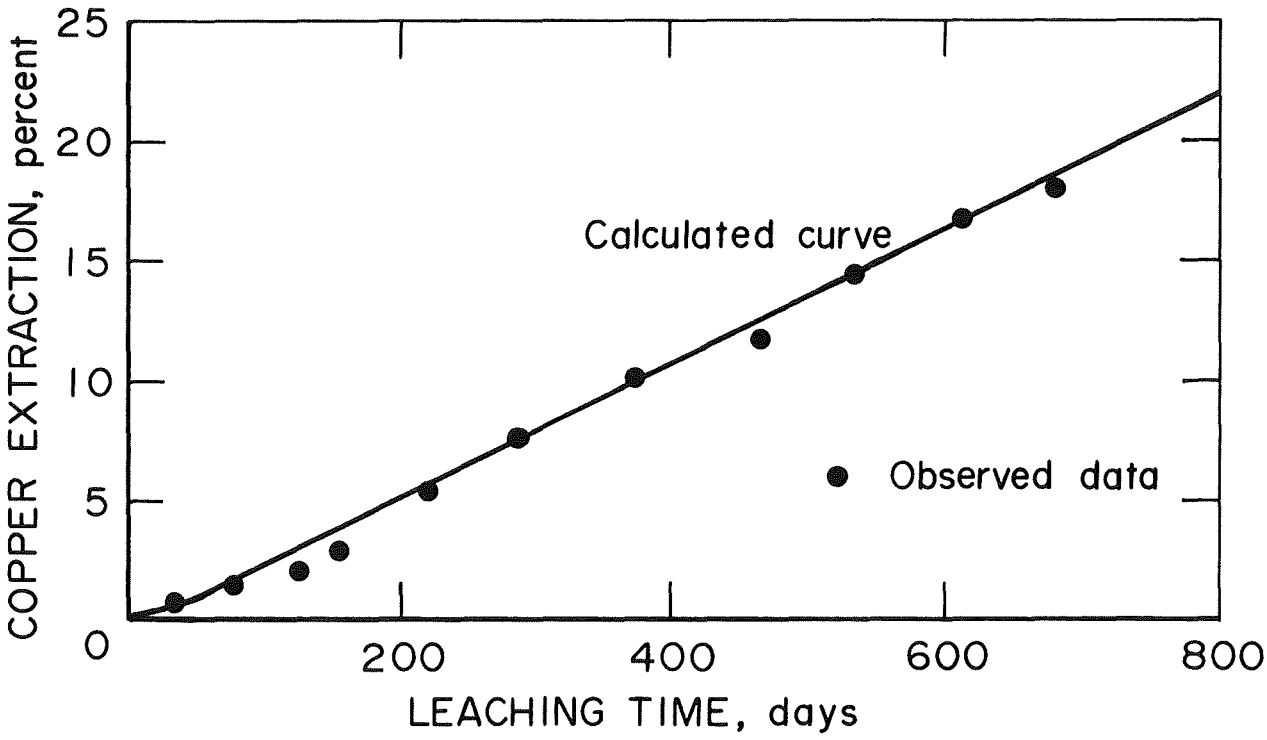

FIGURE 6. - Calculated copper extraction for granitic ore.

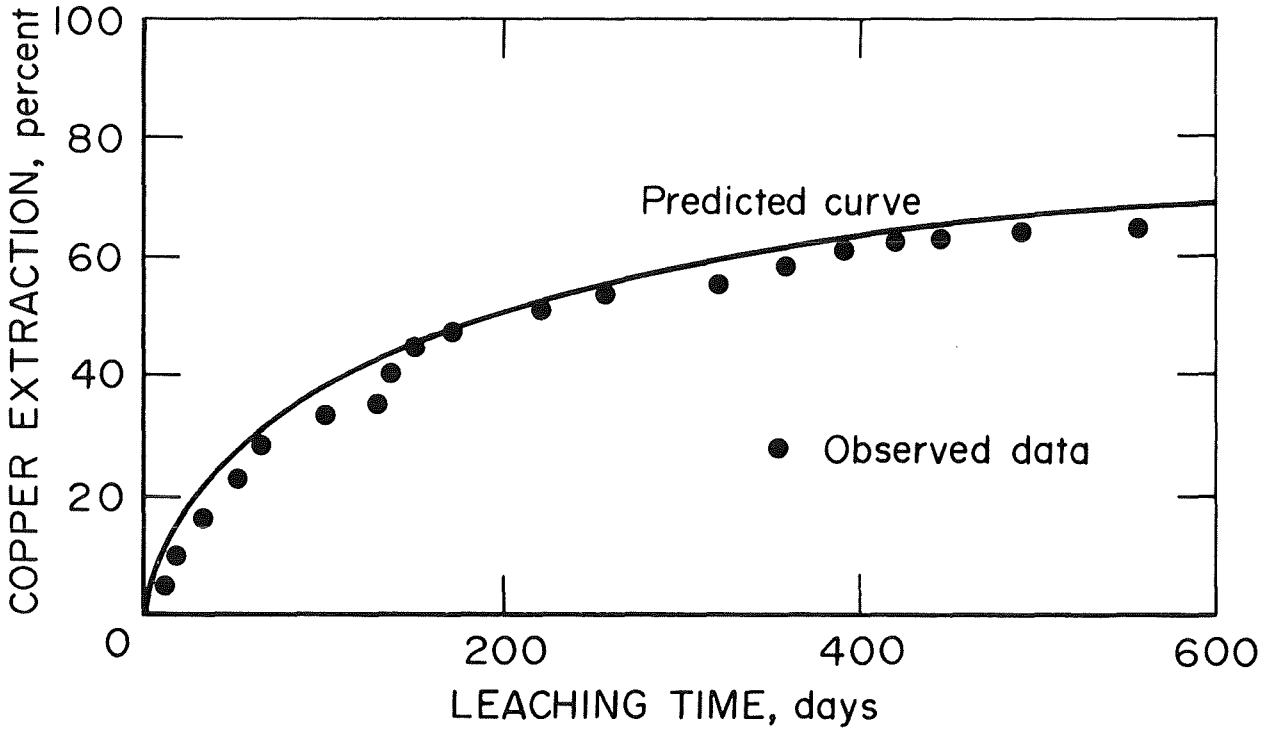

FIGURE 7. - Predicted copper extraction for monzonite ore.

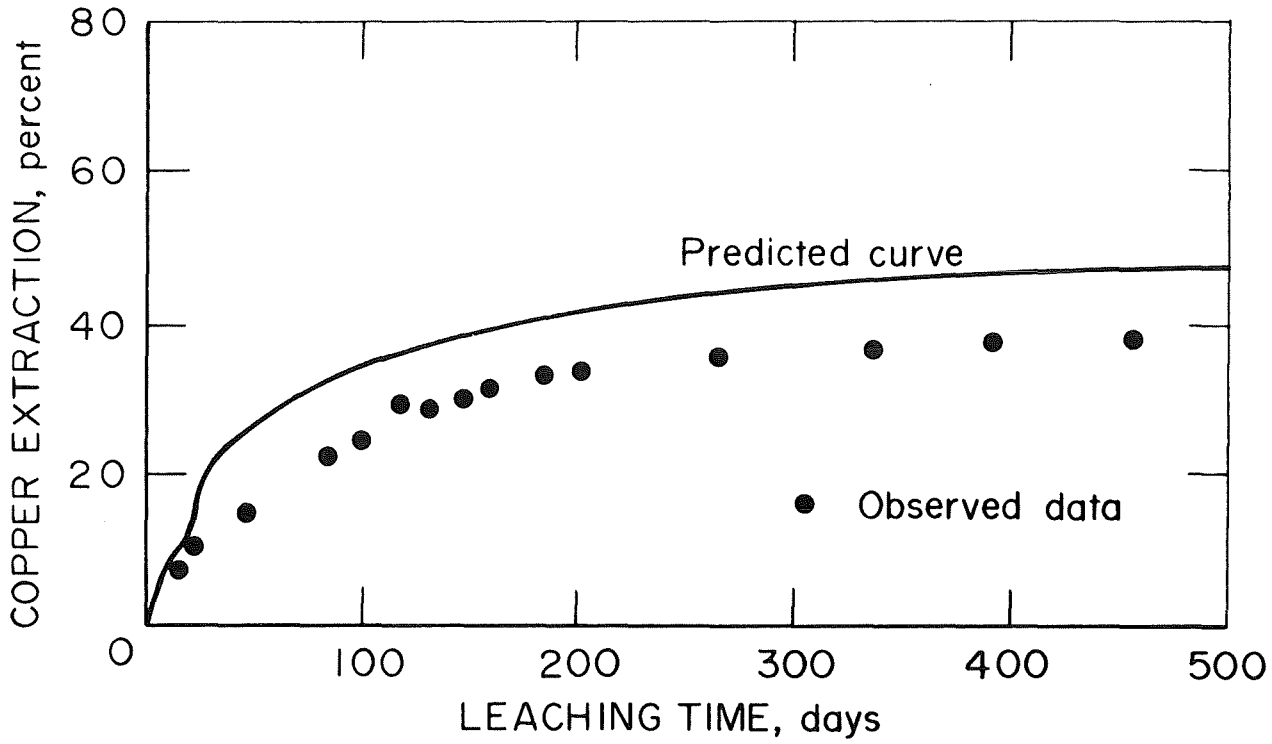

FIGURE 8. - Predicted copper extraction for quartz monzonite I ore.

enabling uniform lixiviant concentration around each ore particle, a basic requisite for the model, was not achieved using unscreened quartz monzonite I ore.

The model calculations demonstrated that effects due to mineralogy, porosity, ore type, and size distribution are accurately simulated using the proposed model based on the continuity equation. The correlation between the predicted extraction curves with the experimental results was very good.

Leaching tests were made with the metasediment and quartz monzonite II ore samples to determine the feasibility of using data from a small-scale leach test to determine the required parameters for the leaching model. Both small-scale [~200-kg (440-pound)] and large-scale [~6,000-kg (13,227-pound)] leaching tests were made with each ore sample, and the experimental data from the smaller test were used to establish the effective diffusivity and late enhancement constant for the model. The established parameters were then used to predict the copper extraction from the larger sample, and the prediction was compared with the experimental data. Figure 9 shows the experimental data and the calculated copper extractions for the small-scale test with the metasediment ore, and figure 10 shows the predicted extractions and experimental extractions for the large-scale test. Since the predictions in figure 10 near the end of the test period were lower than the experimental copper extractions, it was concluded that the late enhancement constant obtained with the small-scale test was too low. This discrepancy occurs because the smaller sized particles are affected less by the late enhancement term (equation 20)

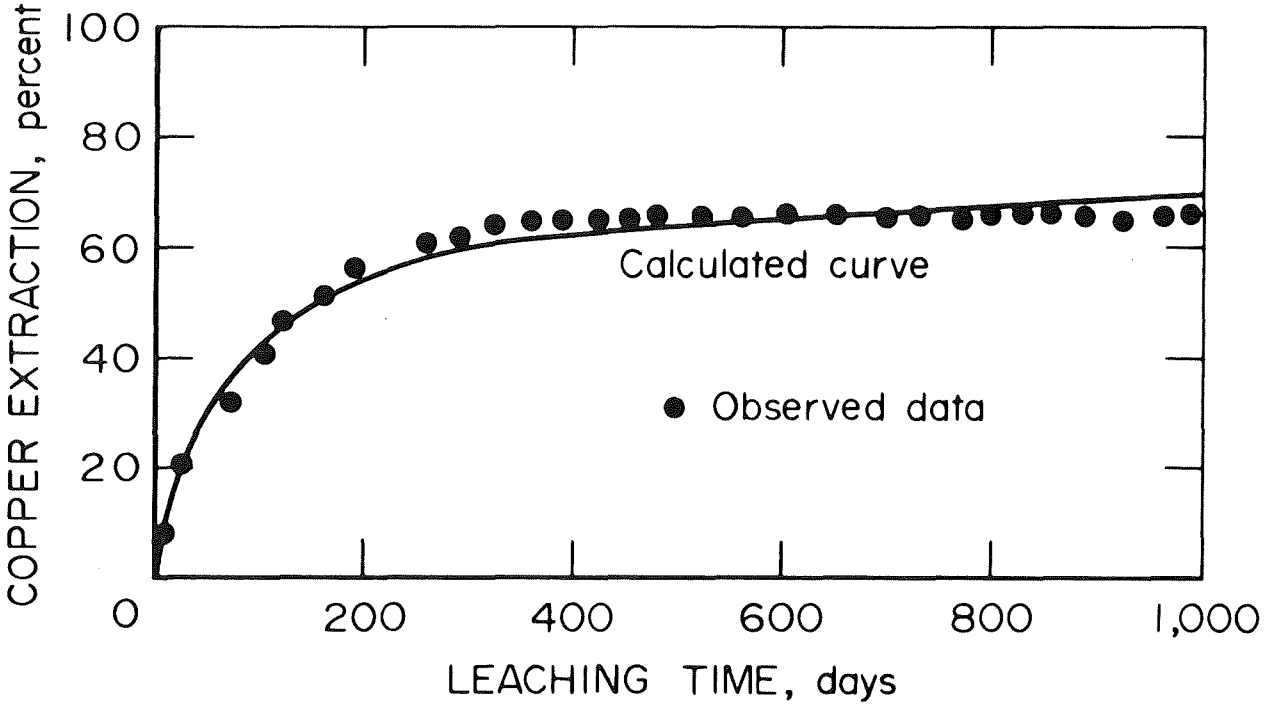

FIGURE 9. - Calculated copper extraction for small-scale test using metasediment ore.

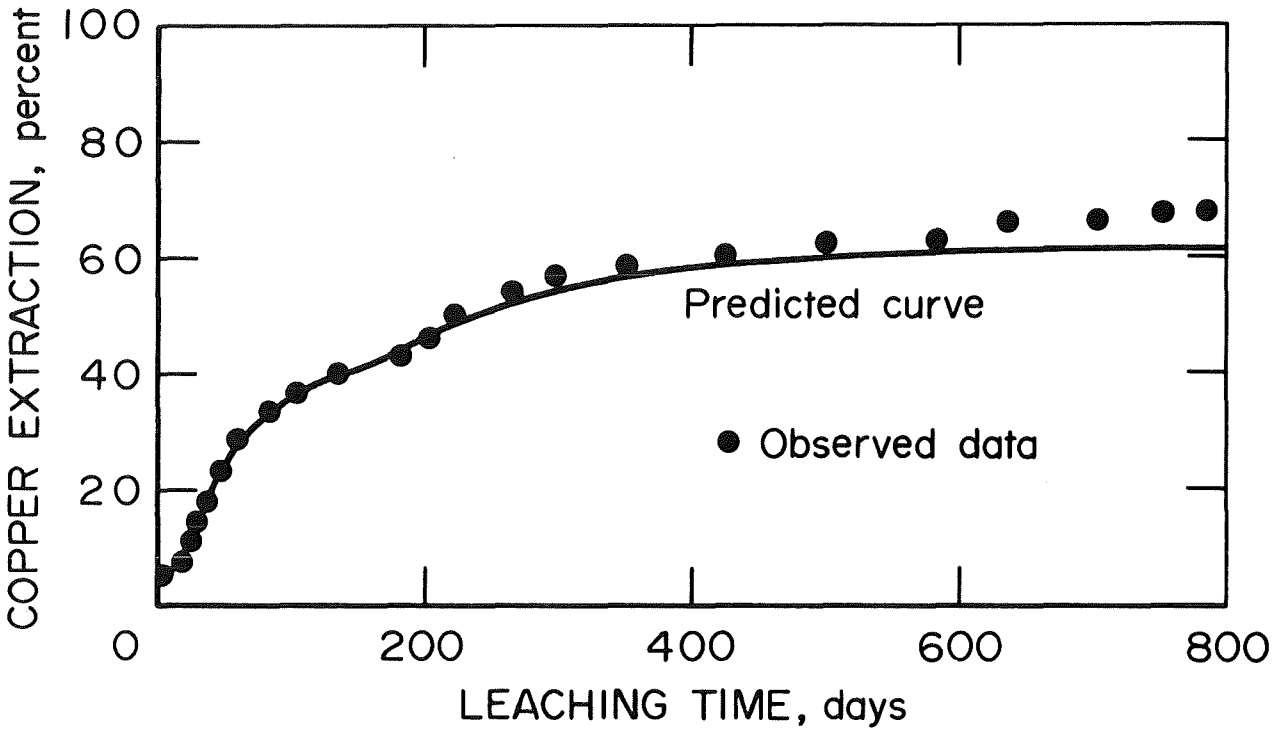

FIGURE 10. - Predicted copper extraction for large-scale test using metasediment ore.

owing to a smaller volume and fewer imperfections. Also, the large number of particles in the large tests make it more representative of the ore sample than the small test. However, in spite of these limitations, the scaleup predictions were always within 7 percent of the observed copper extraction.

Figure 11 shows the experimental data and the calculated copper extractions for the small-scale test with the quartz monzonite II ore, and figure 12 shows the predicted extractions and experimental extraction for the large-scale test. As with the metasediment ore, the prediction of copper extraction from the quartz monzonite II ore was low near the end of the test period. The same reasons for the discrepancy between predicted and observed results are also valid for this case.

The scaleup modeling studies have shown that the model is valid in predicting copper extractions. Application of the model would make laboratory leaching studies less costly if only the small-scale tests are needed for obtaining the leaching parameters required.

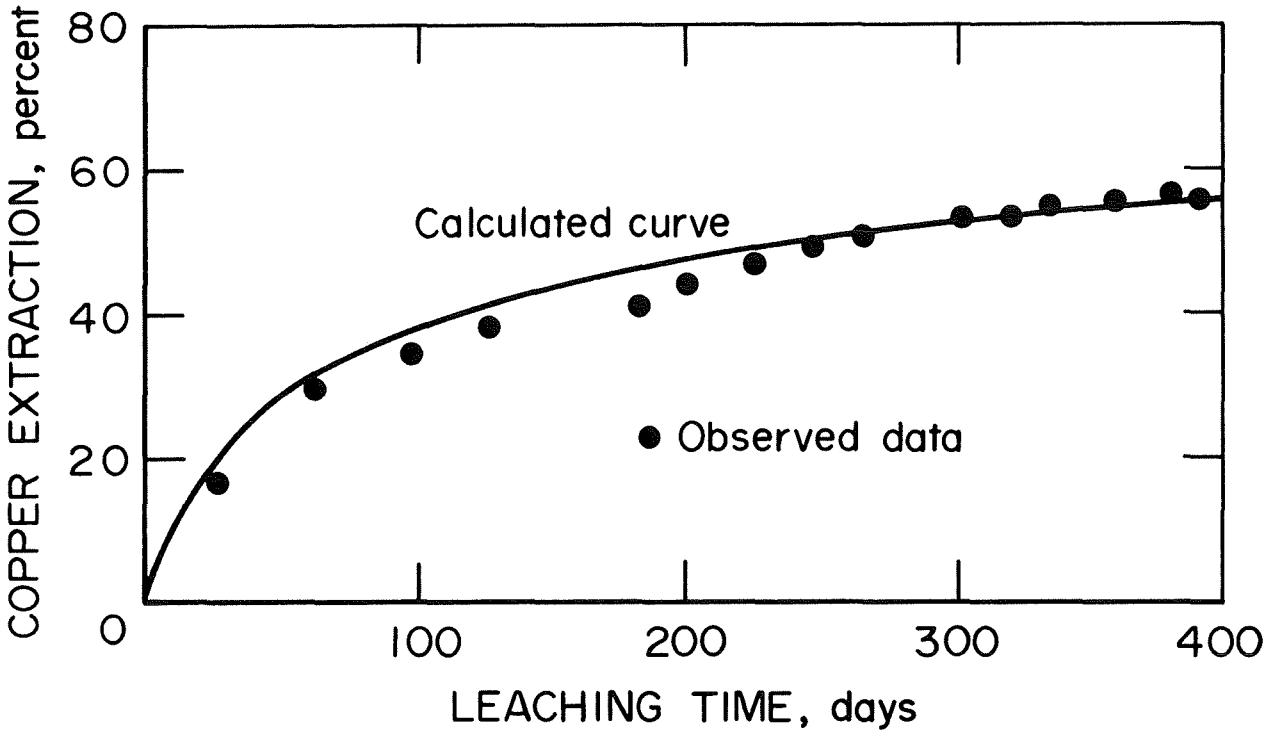

FIGURE 11. - Calculated copper extraction for small-scale test using quartz monzonite II ore.

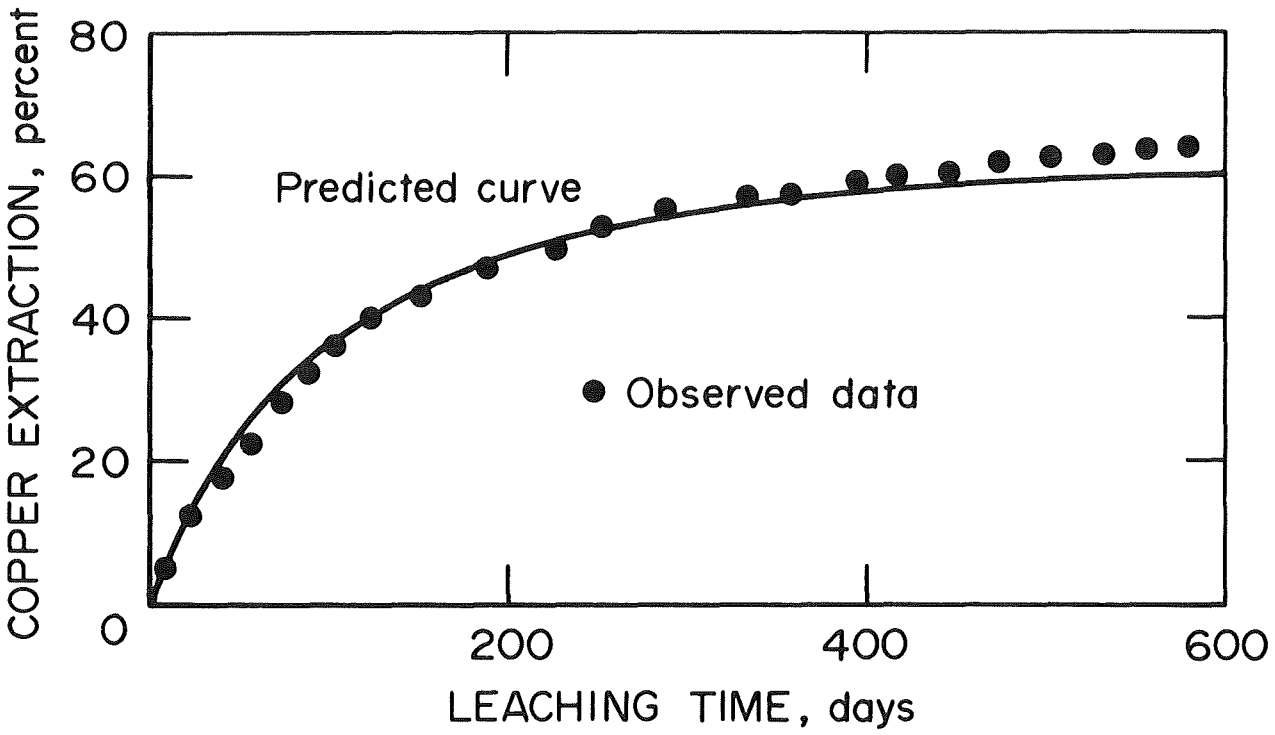

FIGURE 12. - Predicted copper extraction for large-scale test using quartz monzonite II ore.

Comparison of Leaching Parameters for Different Ores

Long-term ore leaching data were used to calculate ore tortuosities using equation 3 relating tortuosity to ore porosity and to both the ordinary and effective diffusivities. The effective ferric diffusivities were determined by curve-fitting techniques using long-term leaching data, and the ordinary diffusivity was estimated by an equation given by Perry (15). Ore porosity was measured by water absorption (ASTM C20-70). Values determined for the five copper ores are shown in table 2. That there was little difference in the tortuosities indicated that there was similar pore structure in each of the ores. After determining ore porosity, effective diffusivities may be easily calculated. This information coupled with the mineral content and size distribution of the ore can be used to predict copper extraction curves for different bulk solution ferric ion concentrations without the need for long-term leach testing.

TABLE 2. - Ore parameters determined from optimization for use in the leaching model

Ore	D_{eo}, 10^{-7} cm^2/sec	D_o, 10^{-7} cm^2/sec	Porosity, pore vol/ore vol	Tortuosity	Late enhancement term, λ
Monzonite.....	6.30	81.2	0.085	1.10	0.01
Quartz monzonite I.	5.79	81.2	.076	1.06	.01
Granitic.....	2.00	81.2	.026	1.06	.01
Metasediment.....	12.13	81.2	.160	1.07	.06
Quartz monzonite II	5.79	81.2	.076	1.06	.01

All ores except the metasediment ore required very little adjustment due to the late enhancement of leaching. With the late enhancement constant, λ, equal to 0.01, the calculated leaching curves are only slightly different from curves generated without adjustment. The value of 0.01 for λ appears to be a suitable average value to use with copper porphyry ores. However, with a sedimentary type ore such as the metasediment ore sample, a larger value must be used to obtain accurate predictions of leaching behavior. The metasediment ore required a late enhancement constant of 0.06, and this high value was justified owing to the weathering noted when the leach residue was examined. The metasediment ore broke down much more extensively than did the other ores tested. A microscopic evaluation of the host rock before leaching could identify the tendency for ores to weather during leaching. Typically such a microscopic examination could show the presence of slate-type host rock formations and of sandstone-type rocks that break down easily when exposed to an acidic solution.

Copper Extraction and Ferric Ion Concentration Profiles

In addition to predicting the composite copper extraction for a large ore sample, the model provides computations that describe the copper extraction and ferric ion concentration profile within individual ore fragments. Analyses of these computed profiles are helpful in determining the mechanisms controlling the leaching kinetics. To illustrate both mechanisms, that is, the intrinsic mineral leaching kinetics and the rate of diffusion of lixiviant through the host rock, copper extraction and ferric ion concentration profiles for fragments of monzonite and granitic ores are depicted graphically in figures 13 and 14, respectively.

In figure 13, the copper extraction profiles for a monzonite ore fragment (which originally contained both chalcocite and chalcopyrite) show that copper extraction abruptly decreases from the outside to the center of ore fragments leached for 72 and 245 days. The steep slope of these copper extraction profiles is due to the rapid leaching of chalcocite and secondary covellite in this zone. The reaction zone, δ, moves inwardly through the ore fragment with time, and the thickness of the zone remains essentially constant. The region on the outward side of the zone is devoid of chalcocite and covellite. In this region chalcopyrite is the only remaining copper mineral, and the slight decrease in the extraction profile reflects the slow leaching character of chalcopyrite. The region on the inward side of the zone is unleached and contains both chalcocite and chalcopyrite. The ferric ion concentration profiles in figure 13 show that the ferric ion concentration is near zero from the inward side of zone δ to the center of the ore fragment. This explains why there was no leaching in this region. However, after 520 days of leaching, the reaction zone for chalcocite and covellite leaching has advanced to the center of the ore fragment and has disappeared. At this time the only remaining copper mineral in the ore fragment is chalcopyrite, which continues to leach at a slow rate. The shape of the copper extraction profiles indicates the mechanism that is controlling the leaching rate. With steeply dipping copper extraction profiles, as with the 72- and 245-day profiles, ferric ions are rapidly consumed and the leaching kinetics are controlled by the diffusion of ferric ions to the leaching zone, δ. However, when steep copper

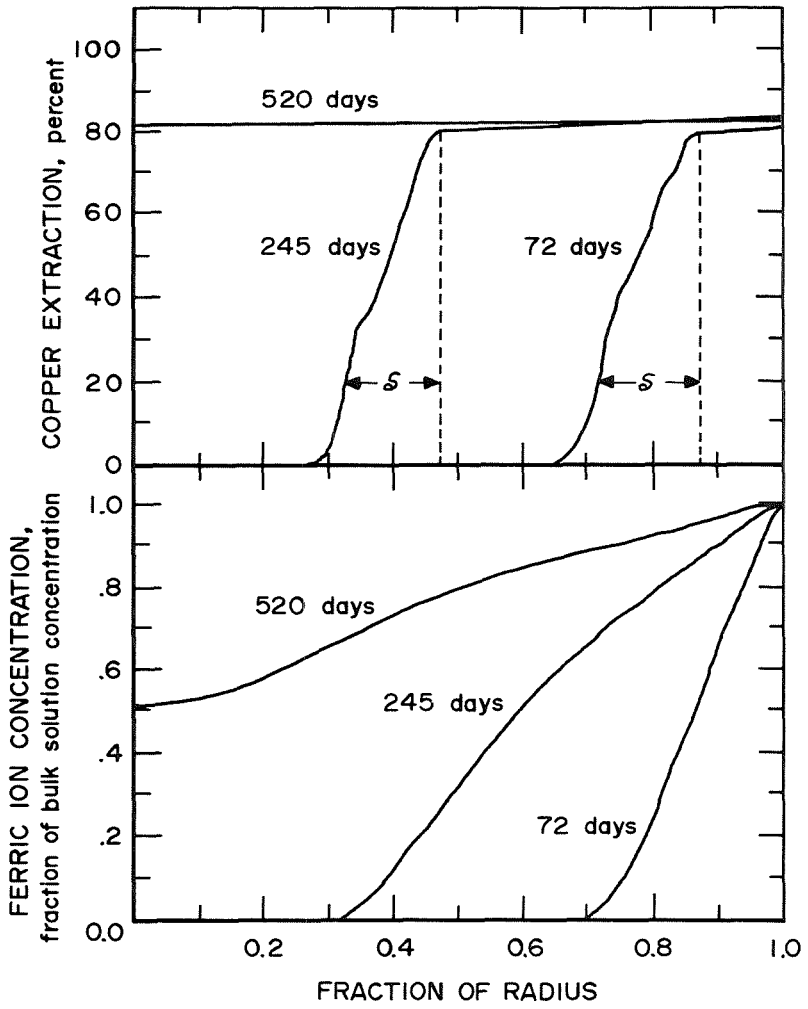

FIGURE 13. - Copper extraction and ferric ion concentration profiles for a 1.54-cm (0.61-inch) radius monzonite ore particle.

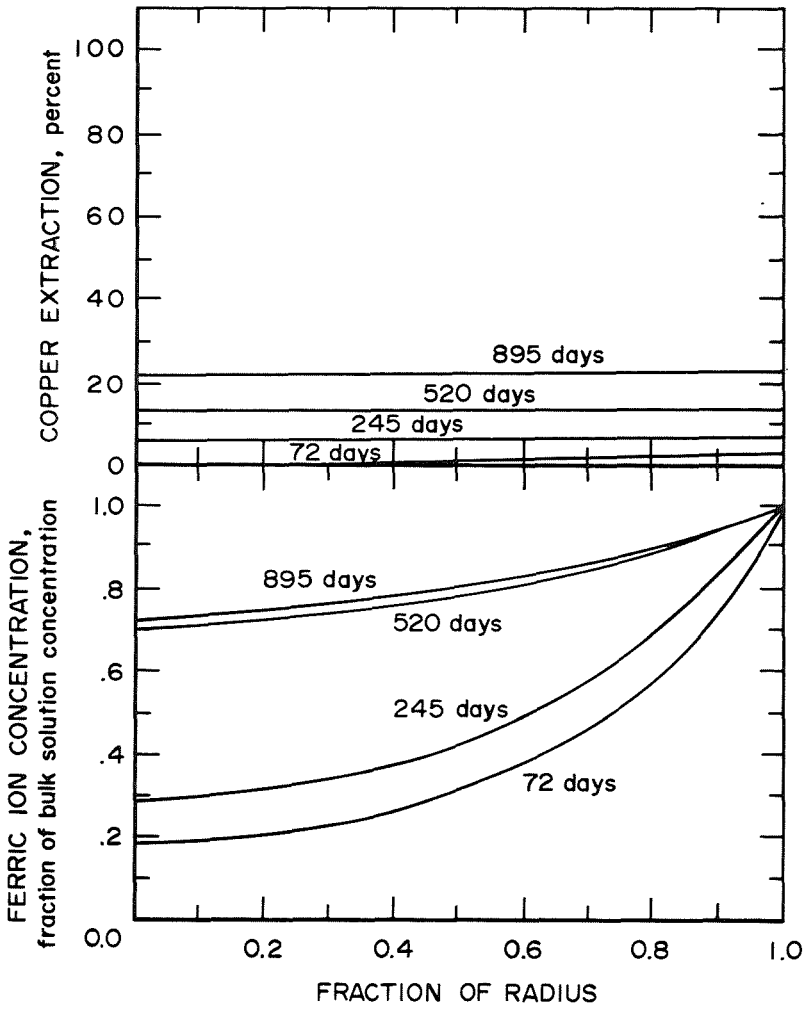

FIGURE 14. - Copper extraction and ferric ion concentration profiles for a 4.96-cm (1.95-inch) radius granitic ore particle.

extraction profiles are not found, such as for the 520-day profile, the leaching kinetics are controlled by the intrinsic leaching rate at the surface of the individual copper minerals. Thus, the mechanism controlling the leaching rate of the 1.54-cm (1/2-inch) monzonite ore fragment changed between the 245th and 520th day of leaching.

Figure 14 shows the copper extraction and ferric ion concentration profiles for an ore fragment from the granitic ore sample. Since this ore contains copper as chalcopyrite only, all the copper extraction profiles are nearly horizontal. As mentioned previously, this type of profile indicates that the leaching kinetics are controlled by the chemical reactions at the surface of the mineral particles. The decrease of ferric ion concentration from the outside to the center of the ore fragment is due chiefly to the reaction of ferric ions with the pyrite contained in the ore. However, by 245 days the ferric ion concentration is high enough in every position in the fragment to give the maximum leaching rate for the chalcopyrite mineral. Hence, the chalcopyrite minerals at the center of the ore fragment leach as fast as the chalcopyrite minerals on the outside surface of the ore fragment.

CONCLUSIONS

The mathematical model used in this study adequately predicts the rate of copper leaching from a large ore sample using acidic-ferric sulfate solution. The accuracy of the prediction was shown to depend on a basic premise--good permeability in the ore bed permitting uniform ferric ion concentration around the ore fragments.

The model is useful in predicting copper recovery rates for large test samples when using leaching parameters obtained from much smaller scale tests. This application of the model would make laboratory leaching studies less costly and more efficient.

The analysis of copper extraction profiles computed by the leaching model is useful in determining whether diffusion of lixiviant through the host rock or chemical leaching at the mineral surfaces is controlling the leaching kinetics.

The ore particle tortuosities were calculated through computer analysis and were similar for each of the four different porphyry copper sulfide ores tested. If the average tortuosity for these four samples is used in the leaching model, then a first approximation of copper extraction can be predicted for laboratory leaching experiments where bulk solution transport is not rate controlling. Also, an approximation to the upper limit of copper extraction from copper sulfide leaching dumps, where bulk solution transport may be rate controlling, can be obtained by using the model predictions.

REFERENCES

1. Bartlett, R. W. A Combined Pore Diffusion and Chalcopyrite Dissolution Kinetics Model for In-Situ Leaching of a Fragmented Copper Porphyry. Internat. Symp. on Hydrometallurgy, AIME, New York, 1972, pp. 331-367.

2. Beckstead, L. W., P. B. Munoz, J. L. Sepulveda, J. A. Herbst, J.D. Miller, F. A. Olson, and M. E. Wadsworth. Acid Ferric Sulfate Leaching of Attritor-Ground Chalcopyrite Concentrates. Proc. Internat. Symp. on Extractive Met. of Copper, v. 2, TMS-AIME, Las Vegas, Nev., Feb. 22-26, 1976, Ch. 31, pp. 611-632.

3. Braithwaite, J. W. Simulated Deep Solution Mining of Chalcopyrite and Chalcocite. Unpublished Ph.D. Dissertation, Univ. Utah, Salt Lake City, Utah, 1976; available for inspection at the University of Utah library.

4. Braun, R. L., A. E. Lewis, and M. E. Wadsworth. In-Place Leaching of Primary Sulfide Ores: Laboratory Leaching Data and Kinetics Model. Met. Trans., AIME, v. 5, August 1974, pp. 1717-1726.

5. Dutrizac, J. E., and R. J. C. MacDonald. The Kinetics of Dissolution of Covellite in Acidified Ferric Sulfate Solutions. Can. Met. Quart., v. 13, 1974, pp. 423-433.

6. Dutrizac, J. E., R. J. C. MacDonald, and T. R. Ingraham. The Kinetics of Dissolution of Synthetic Chalcopyrite in Aqueous Acidic Ferric Sulfate Solutions. Met. Trans., AIME, v. 245, 1969, p. 955-959.

7. Erdey-Gruz, T. Transport Phenomena in Aqueous Solutions. John Wiley & Sons, New York, 1974, p. 146.

8. Harned, H. S., and B. B. Owen. The Physical Chemistry of Electrolytic Solutions. Reinhold Pub. Corp., New York, 1950, p. 428.

9. Hattox, E. M., and T. DeVries. The Thermodynamics of Aqueous Indium Sulfate Solutions. J. Am. Chem. Soc., v. 58, 1936, pp. 2126-2129.

10. Jones, J. L., and E. Peters. The Leaching of Chalcopyrite With Ferric Sulfate and Ferric Chloride. Proc. Internat. Symp. on Extractive Met. of Copper, v. 2, TMS-AIME, Las Vegas, Nev., Feb. 22-26, 1976, Ch. 3, pp. 633-653.

11. Madsen, B. W., M. E. Wadsworth, and R. D. Groves. Application of a Mixed Kinetics Model to the Leaching of Low-Grade Copper Sulfide Ores. Trans. SME/AIME, v. 258, March 1975, pp. 69-74.

12. Marcontonio, P. J. Chalcocite Dissolution in Acidic Ferric Sulfate Solutions. Unpublished Ph.D. Dissertation, Univ. Utah, Salt Lake City, Utah, 1976; available for inspection at the University of Utah library.

13. Mathews, C. T., and R. G. Robins. The Oxidation of Iron Disulphide by Ferric Sulfate. Australian Chem. Eng., August 1972, pp. 21-25.

14. Munoz, P. B., J. D. Miller, and M. E. Wadsworth. Reaction Mechanism for the Acid Ferric Sulfate Leaching of Chalcopyrite. Met. Trans., AIME, v. 10B, June 1979, pp. 149-158.

15. Perry, J. H. Chemical Engineers Handbook. McGraw-Hill Book Co., Inc., New York, 1963, sec. 14, pp. 23-24.

16. Roman, R. J., B. R. Benner, and G. W. Becker. Diffusion Model for Heap Leaching and Its Application to Scale-Up. Trans. SME/AIME, v. 256, September 1974, pp. 247-252.

17. Schroeder, H. J. Copper. BuMines Mineral Commodity Profiles, 1977, p. 13.

18. Smith, J. M. Chemical Engineering Kinetics. McGraw-Hill Book Co., Inc., New York, 1970, p. 414.

19. Sohn, H. Y., and J. Szekely. A Structural Model for Gas-Solid Reactions With a Moving Boundary--Part III. Chem. Eng. Sci., v. 27, 1972, pp. 763-778.

20. Taggart, A. F. Handbook of Mineral Dressing. John Wiley & Sons, Inc., New York, 1945, sec. 19, p. 146.

APPENDIX A.--LIST OF SYMBOLS

c = Concentration, moles/cm^3.

D_o = Ordinary ferric ion diffusion coefficient, cm^2/sec.

D_{eff} = Effective ferric ion diffusion coefficient, cm^2/sec.

D_{eo} = Effective ferric ion diffusion coefficient at infinite dilution, cm^2/sec.

F_i = Fraction of the copper contained in the ith size interval.

$[Fe^{+3}]$ = Ferric ion concentration in the solution, moles/cm^3.

$[Fe_{tot}]$ = Total iron concentration in the solution, moles/cm^3.

G = Ore grade, grams copper/gram ore.

H^+ = Hydrogen ion concentration, moles/cm^3.

j = Subscript denoting position within ore fragment.

K = Largest theoretical ore particle diameter in ore sample, cm.

k = Subscript denoting mineral type.

k^I = Rate constant for first-stage leaching of chalcocite = $2.15 \times 10^3 \exp(2790/1.98T)$.

k^{II} = Rate constant for second-stage leaching of chalcocite = $2.10 \times 10^{10} \exp(-18000/1.98T)$.

k^{III} = Rate constant for leaching natural covellite = $1.05 \times 10^4 \exp(17780/1.98T)$.

k^{IV}, k^V = Rate constants for leaching chalcopyrite.

L = Number of size intervals.

MW_{Cu} = Molecular weight of copper.

N = Number of positions (denoted by subscript j) within the ore fragment.

P = Constant used in size distribution calculations = $(s/K)^{(1/L)}$.

Q = Smallest ore particle diameter in ore sample, cm.

q_k = The order dependence of the leaching rate of mineral k on ferric ion activity.

r = Particle radius, cm.

r_o = Initial mineral particle of ore fragment radius, cm.

s = Smallest theoretical ore particle diameter in ore sample, cm.

S = Surface area of pyrite, cm^2/gram.

T = Temperature, K.

t = Time, sec.

V = Volume of ore particle, cm^3.

W = Weight of pyrite, grams.

X = Ore particle diameter, cm.

Y = Accumulative weight fraction passing size x.

Z = Slope of theoretical line on Schuhmann plot.

α = Fraction of copper reacted.

α_ν = Fraction of copper reacted for ore particle at time level ν.

α' = Fraction of copper reacted during first-stage leaching of chalcocite.

α'' = Fraction of copper reacted during second-stage leaching of chalcocite.

γ = Activity coefficient for ferric ion.

Δr = Thickness of concentric shell, cm.

∇^2 = Mathematical operator dependent on particle geometry.

ε = Ore porosity, pore volume/fragment volume.

λ = Constant affecting late enhancement of leaching.

ν = Subscript denoting time level.

ρ = Ore density, grams/cm^3.

ΣR_k = Consumption rate of ferric ion, moles/sec/fragment volume.

σ_k = Stoichiometry factor, moles ferric ion/mole copper extraction from mineral k.

τ = Tortuosity, ratio of the actual diffusion path length to the perpendicular path length.

ϕ_ν = Shape factor of time level ν.

$(\varepsilon/\tau)_o$ = Initial ratio of porosity to tortuosity.

APPENDIX B.--COMPUTER PROGRAM

The computer listing of the Fortran V program used to numerically solve the continuity ore mathematical model is given in this appendix. A brief description of the function of the main program and each subroutine along with the definition of the variable names used in the Fortran V program precede the actual program listing.

The MAIN program was used for data input, variable initialization, subroutine access, and the output of results. Subroutine CONSOL calculated the ferric ion profile throughout the ore fragment at any given time. Subroutine RATE advanced the time by calculating new copper fraction extracted profiles and overall copper fraction extracted values by numerically solving the appropriate differential rate equations by Euler's method. Subroutine SIZE calculated the size distribution of the sample giving a set of ordered pairs (r_{Io}, F_I) where r_{Io} is an average radius of a size interval containing the fraction of the total copper F_I.

The meaning of variable names used in the computer program listed below are as follows:

NRUNS : the number of computer runs,

NAME : the name of the ore sample,

T1 : initial time increment,

T5 : cutoff time for two empirical ferric ion concentration curves,

DEFE : the effective diffusivity for ferric ions,

G6 : (ore density) *2,

N-1 : the number of concentric shells the ore fragment was broken into,

TT1 : rate constant for first-stage leaching of chalcocite,

TT2 : rate constant for second-stage leaching of chalcocite,

TT3 : rate constant for leaching of chalcopyrite,

TT4 : rate constant for leaching of natural covellite,

S5 : fraction of copper contained as chalcocite,

S6 : fraction of copper contained as bornite,

S7 : fraction of copper contained as covellite,

S8 : fraction of copper contained as other minerals,

S1 : fraction of copper available in first-stage leaching of chalcocite,

S2 : fraction of copper available in second-stage leaching of chalcocite,

S3 : fraction of copper available in chalcopyrite,

S4 : fraction of copper available in natural covellite,

INCT : the time print increment (for profiles),

INCR : the radius print increment (for profiles),

INCAT : the time print and punch increment (for α and time),

INCTP : the card punch increment (for profiles),

F : shape factor (f),

H1-H9 : regression constants for empirical ferric ion concentration after cutoff time,

B1-B8 : regression constants for empirical ferric ion concentration before cutoff,

TMAX : maximum time,

PCPR : pyrite/chalcopyrite mole ratio.

EST : initial temporary ferric ion activity expansion point equals EST * Fe^{+3}_{B},

XX : order dependence of second-stage leaching of chalcocite on ferric ion activity,

PHI : initial shape factor (ϕ_o),

XLAMB : λ,

DELT : Δt,

DELR : Δr,

AO : slope on Gaudin plot (Z),

SO : smallest diameter ore particle in sample (S),

CO : largest diameter ore particle in sample,

C9 : largest diameter ore particle in screened sample (K),

L : number of size fractions (L),

SL1, SL2: regression constants to describe the copper grade as a function of particle radius,

RAVG(J) : average radius of size interval J,

GRAD(J) : grade of copper of radius J,

WT(J) : weight fraction of size interval J,

S(J) : fraction of the copper in interval J,

A33(J) : fraction of chalcopyrite reacted at position j at time t,

A44(J) : fraction of natural covellite reacted at position j at time t ,

CO(J) : activity of ferric ions at position j at time t,

ALPHA(J): fraction of copper extracted at position j at time t,

ALPRE : overall fraction copper extracted for one particle size at time t,

T(I) : time (t) at time level I,

COB : concentration of ferric ions in bulk solution,

ACT : activity coefficient,

ENH : changing shape factor (ϕ),

TOTEXT : total fraction copper extracted from entire sample at time t.

To be helpful to a program user, the order and format of the input is provided in table B-1, and the computer program listing follows.

TABLE B-1. - Computer input data and format

Card	Variable name	Description of variable	Read format
1.....	NRUNS.....	Number of computer runs.....	I10
2.....	NAME.....	Name of ore sample.....	20A4
3.....	T1, T5.....	Initial time increment, cutoff time (days).....	2F10.5
4.....	DEFE, G6.....	Effective diffusivity, ore density *2.....	2F10.5
5.....	N.....	Number of shells + 1.....	I10
6.....	TT1, TT2, TT3, TT4.....	Rate constants.....	4F10.5
7.....	S5, S6, S7, S8.....	Copper distribution.....	4F10.5
8.....	INCT, INCR, INCAT, INCTP	Print and punch increments.....	4I10
9.....	F.....	Shape factor (f).....	F10.5
10.....	H1-H8.....	Ferric iron regression constants.....	8E10.4
11.....	H9.....	Ferric iron regression constant.....	E10.4
12.....	B1-B8.....	Ferric iron regression constants.....	8E10.4
13.....	TMAX.....	Maximum time (days).....	F10.4
14.....	PCPR.....	Pyrite/chalcopyrite mole ratio.....	F10.4
15.....	EST.....	Taylor series expansion constant.....	F10.4
16.....	XX.....	Ferric order dependency of second-stage chalcocite.	2F10.4
17.....	PHI, XLAMB.....	Initial shape factor (ϕ_o), λ.....	2F10.4
18.....	SL1, SL2.....	Regression constants for grade versus size.....	2F10.4
19.....	AO, SO, CO, C9, L.....	Size distribution parameters.....	4F10.2, I40

MAIN PROGRAM

```
      COMMON/JJJ/N,I,ALPRE,CO,DELT,ST1,ST2,ST3,PRE,COB,B,TT,
     CA1P,A2P,A2R,ALPHA,EST,Z,F,PRESP,RAVG,GRAD,TOTEXT,T,S1,
     CS2,L,S,K,PCPR,S4,S3,ST4,A44,A33,XX,ACT
      DIMENSION CO(250),ALPHA(250),B(250),Z(250),TOTEXT(900)
     C,T(900),RAVG(25),GRAD(25),S(25),A44(250),A33(250),NAME
     C(20)
    1 FORMAT(8E10.4)
   20 FORMAT (16X,'J=',I2,'      J=',I2,'      J=',I2,6X,
     C,'J=', I2,'      J=',I2,'      J=',I2,'      J=',I2,6X
     C,'J=',I2)
   21 FORMAT(8X,'TIME',3X,'AFE(',I2,')   AFE(',I2,')   AFE('
     C,I2,')   AFE(',I2,')   AFE(',I2,')   AFE(',I2,')',3X,
     C'AFE(',I2,')   AFE(',I2,')   AFE(',I3,')   AFE(',I3,
     C')   AFE(',I3,')   AFE(',I3,')')
   22 FORMAT(8X,'TIME',3X,'ALP(',I2,')   ALP(',I2,')   ALP('
     C,I2,')   ALP(',I2,')   ALP(',I2,')   ALP(',I2,')',3X,
     C'ALP(',I2,')   ALP(',I2,')   ALP(',I3,')   ALP(',I3,
     C')   ALP(',I3,')   ALP(',I3,')')
   23 FORMAT (7X,'*****   *******   *******   *******',3X,
     C'*******   *******   *******   *******   *******',3X,
     C'*******   *******   *******   *******',//)
   26 FORMAT(8X,'TIME',3X,'CUS(',I2,')   CUS(',I2,')   CUS('
     C,I2,')   CUS(',I2,')   CUS(',I2,')   CUS(',I2,')',3X,
     C'CUS(',I2,')   CUS(',I2,')   CUS(',I3,')   CUS(',I3,
     C')   CUS(',I3,')   CUS(',I3,')')
   27 FORMAT(8X,'TIME',3X,'CPR(',I2,')   CPR(',I2,')   CPR('
     C,I2,')   CPR(',I2,')   CPR(',I2,')   CPR(',I2,')',3X,
     C'CPR(',I2,')   CPR(',I2,')   CPR(',I3,')   CPR(',I3,
     C')   CPR(',I3,')   CPR(',I3,')')
    2 FORMAT(8F10.5)
    5 FORMAT (3X,F8.4,1X,12E10.3)
   10 FORMAT(8I10)
   16 FORMAT(3X,'ACT COFF',//)
   17 FORMAT(1H1,1X,'ALPHA TOTAL',5X,'TIME(DAYS)')
   18 FORMAT(F8.4,F17.4)
   24 FORMAT(//,5X,'IRON DIFFUSIVITY=',E9.4,' SQCM/DAY',5X,'
     C PARTICLE RADIUS=',F8.4,' CM',//)
    6 FORMAT(3X,F8.4,1X,12E10.3   )
   28 FORMAT(1H1)
   31 FORMAT(//,5X,'    CU2S=',F8.4)
   32 FORMAT(   5X,'     CUS=',F8.4)
   33 FORMAT(   5X,' BORNITE=',F8.4)
   34 FORMAT(   5X,'  CUFES2=',F8.4)
   35 FORMAT(//,5X,' LAMBDA2=',F8.4)
   36 FORMAT(//,5X,' PHI I0 =',F8.4)
   55 FORMAT(1H1)
```

```
817 FORMAT(20A4)
818 FORMAT(2X,20A4)
825  FORMAT(' PYRITE/CHALCOPYRITE RATIO= ', F8.3)
826 FORMAT(2X,'ORIGINAL TIME INCREMENT=', F10.4)
827 FORMAT(2X,'BREAK POINT TIME (FE+3)=', F10.4)
828 FORMAT(2X,'DENSITY*SIGMA=', F10.4)
829 FORMAT(2X,'RATE CONSTANT (   CU2S)  =',  F10.4)
830 FORMAT(2X,'RATE CONSTANT (  CUS  )  =',  F10.4)
831 FORMAT(2X,'RATE CONSTANT (NAT CUS)  =',  F10.4)
832 FORMAT(2X,'RATE CONSTANT (CUFES2 )  =',  F15.6)
837 FORMAT(2X,'SHAPE FACTOR=',F10.2,'2=SPHERE;1=CYLINDER;0
   C=FLAT PLATE')
900 FORMAT(10F8.4)
901 FORMAT(F8.3,9E8.3)
902 FORMAT(10E8.3)
    READ10,NRUNS
    DO45 NQ=1,NRUNS
    READ(5,817) NAME
    READ2,T1,T5
    READ2,DEFE,G6
    READ 10,N
    READ2,TT1,TT2,TT3,TT4
    READ2,S5,S6,S7,S8
    READ10,INCT,INCR,INCAT,INCTP
    READ2,F
    READ 1,H1,H2,H3,H4,H5,H6,H7,H8
    READ1,H9
    READ 1,B1,B2,B3,B4,B5,B6,B7,B8
    READ2,   TMAX
    READ2,PCPR
    READ2,EST
    READ2,XX
    READ2,PHI,XLAMB
    WRITE(7,818)NAME
    WRITE(7,900) TT3,DEFE
    PRINT 55
    WRITE(6,818) NAME
    PRINT 36, PHI
    PRINT 35, XLAMB
    PRINT 825, PCPR
    S1=0.4*S5+0.25*S6
    S2=0.6*S5+0.75*S6
    S4=S7+S8
    S3=1.0-S1-S2-S4
    PRINT 32,S7
    PRINT 31,S5
    PRINT 33,S6
    PRINT 34,S3
    PRINT 826,T1
    PRINT 827,T5
    PRINT 828,G6
    PRINT 829,TT1
    PRINT 830,TT2
```

```
      PRINT 831,TT4
      PRINT 832,TT3
      PRINT 837,F
      TT1=TT1*S1
      TT2=TT2*S2
      TT3=TT3*S3
      TT4=TT4*S4
      B(1)=1.
      Z(N)=0.
      III=INCT
      MM=N-1
      PRE=1./((N-1)*(N-1))
      PRESP=PRE/(2*(N-1))
      CALL SIZE
      DO7 I=2,900
      TOTEXT(I)=0.0
    7 CONTINUE
      TOTEXT(1)=0.0
      DO 66 K=1,L
      A1P=S1
      A2P=S1+S2
      III=1
      IV=1
      RAD=RAVG(K)
      DELR=RAD/(N-1)
      T(1)=0.0
      TT=1000.*DELR*DELR*G6*GRAD(K)/(DEFE*100.*63.54)
      TTZ=TT
      B(1)=1.0
      Z(N)=0.0
      MM=N-1
      DO 4 J=2,MM
      Z(J)=(1.-F/(2.*(J-1)))
    4 B(J)=(1.+F/(2.*(J-1)))
      PRINT 28
      WRITE(6,818) NAME
      PRINT 24,DEFE,RAVG(K)
      PRINT 20,(J,J=1,N,INCR)
      PRINT 21,(J,J=1,N,INCR)
      PRINT 22,(J,J=1,N,INCR)
      PRINT26,(J,J=1,N,INCR)
      PRINT27,(J,J=1,N,INCR)
      PRINT 16
      PRINT 23
      DO 8 J=1,N
      A33(J)=0.0
      A44(J)=0.0
      CO(J)=0.
    8 ALPHA(J)=0.
      DELT=T1
      DO9 I=2,900
      ALPRE=0.0
      T(I)=T(I-1)+DELT
```

```
      IF(T(I).GE. TMAX) GO TO 66
      IF(T(I).GT.T5)GOTO 70
      COB=B1+B2*T(I)+B3*T(I)**2.+B4*T(I)**3.+B5*T(I)**4.+B6*
     CT(I)**5.+B7*T(I)**6.+B8*T(I)**7.
      GOTO75
   70 COB=H1+H2*T(I)+H3*T(I)**2.+H4*T(I)**3.+H5*T(I)**4.+H6*
     CT(I)**5.+H7*T(I)**6.+H8*T(I)**7.+H9*T(I)**8.
   75 COB=COB/55.85
      COB=ABS(COB)
      ACT=EXP(-1.3734-7.5801*COB**0.5+4.8712*COB)
      COB=COB*ACT
      CO(N)=COB
      ST1=TT1
      ST2=TT2
      ST3=TT3/ACT
      ST4=TT4/ACT
      CALL CONSOL
      CALL RATE
      ENH=PHI**2. -.6666*XLAMB*ALPRE*(RAVG(K)**3.)
      IF(ENH .LE. 0.0)ENH=0.17**2.
      ENH=SQRT(ENH)
      IF(ENH .LT. 0.17)ENH=0.17
      TT=TTZ*ENH
      TOTEXT(I)=TOTEXT(I)+ALPRE*S(K)
      DELT=T1/10.  + DELT
      IF(III.EQ.INCT)GOTO 15
      GOTO25
   15 PRINT5,T(I),(CO(J),J=1,N,INCR)
      PRINT5,ALPRE,(ALPHA(J),J=1,N,INCR)
      PRINT5,T(I),(A44(J),J=1,N,INCR)
      PRINT6,T(I),(A33(J),J=1,N,INCR)
      PRINT 5,ACT
      IF(IV.EQ.INCTP)GOTO 955
      GO TO 956
  955 WRITE(7,902)COB
      WRITE(7,901)T(I),(CO(J),J=1,9)
      WRITE(7,902)(CO(J),J=10,19)
      WRITE(7,902)(CO(J),J=20,29)
      WRITE(7,902)(CO(J),J=30,39)
      WRITE(7,902)(CO(J),J=40,49)
      WRITE(7,902)(CO(J),J=50,56)
      WRITE(7,900)(ALPHA(J),J=1,10)
      WRITE(7,900)(ALPHA(J),J=11,20)
      WRITE(7,900)(ALPHA(J),J=21,30)
      WRITE(7,900)(ALPHA(J),J=31,40)
      WRITE(7,900)(ALPHA(J),J=41,50)
      WRITE(7,900)(ALPHA(J),J=51,56)
      IV=1
      GOTO 980
  956 IV=IV+1
  980 III=1
      GOTO9
   25 III=III+1
```

```
 9 CONTINUE
66 CONTINUE
   PRINT 17
   IQ=I
   DO45 K=1,IQ,INCAT
   PRINT18,TOTEXT(K),T(K)
   WRITE(7,900) TOTEXT(K),T(K)
45 CONTINUE
   END
```

SUBROUTINE SIZE

```
      SUBROUTINE SIZE
      COMMON/JJJ/N,I,ALPRE,CO,DELT,ST1,ST2,ST3,PRE,COB,B,TT,
     CA1P,A2P,A2R,ALPHA,EST,Z,F,PRESP,RAVG,GRAD,TOTEXT,T,S1,
     CS2,L,S,K,PCPR,S4,S3,ST4,A44,A33,XX,ACT
      DIMENSION RAVG(25),GRAD(25),WT(25),S(25),CO(250),B(250
     C),Z(250),ALPHA(250),TOTEXT(900),T(900),A44(250),A33(25
     C0)
  200 FORMAT(4F10.2,I40)
  201 FORMAT(8F10.4)
  202 FORMAT(5X,'AVERAGE RADIUS(CM)',5X,'GRADE(PERCENT)',5X,
     C'WT(FRACTION)',5X,'CU DIST(FRACTION)')
      READ 201, SL1,SL2
      READ 200,A0,S0,C0,C9,L
      E=0.0
      W6=0.0
      IF(S0.GT.0.05)GOTO 121
      S0=S0+0.05
  121 Z0=(S0/C0)**(1.0/L)
      IF(S0.GT.0.06)GOTO 124
      S0=S0-0.05
  124 P0=(C9/C0)**A0-(S0/C0)**A0
      X2=C9
      DO 950 J=1,L
      X1=X2
      X2=X1*Z0
      R1=X1/2.0
      R2=X2/2.0
      RAVG(J)=SQRT((R1*R1+R2*R2)/2.)
      GRAD(J )=SL1-SL2*RAVG(J)
      Y1=(X1/C0)**A0
      Y2=(X2/C0)**A0
      WT(J)=(Y1-Y2)/P0
  950 CONTINUE
      PRINT 202
      DO 805 J=1,L
      W6=W6+WT(J)
      E=E+GRAD(J)*WT(J)
  805 CONTINUE
      IF((ABS(W6-1.)).LE.0.005)GOTO 195
      U2=1.-W6
      WT(L)=U2+WT(L)
      RAVG(L)=(RAVG(L-1)+S0)/2.0
  195 DO810 J=1,L
      S(J)=GRAD(J)*WT(J)/E
      PRINT 203,RAVG(J),GRAD(J),WT(J),S(J)
  203 FORMAT(2F19.4,F17.4,F21.4)
```

```
  810 CONTINUE
      RETURN
      END
```

SUBROUTINE CONSOL

```
      SUBROUTINE CONSOL
      COMMON/JJJ/N,I,ALPRE,CO,DELT,ST1,ST2,ST3,PRE,COB,B,TT,
     CA1P,A2P,A2R,ALPHA,EST,Z,F,PRESP,RAVG,GRAD,TOTEXT,T,S1,
     CS2,L,S,K,PCPR,S4,S3,ST4,A44,A33,XX,ACT
      DIMENSION D(250),Z(250),A(250),B(250),W(250),G(250),Q(
     C250),CO(250),COT(250),COTQ(250),ALPHA(250),RAVG(25),GR
     CAD(25),TOTEXT(900),T(900),S(25),A44(250),A33(250)
      W(1)=-1.
      A(1)=-1.
      D(1)=0.
      A(N)=1.
      D(N)=COB
      G(1)=0.
      DO 1 J=1,N
      IF(A44(J).GE..99)A44(J)=1.0
      IF(A33(J).GE..99)A33(J)=1.0
    1 COT(J)=COB*EST
      MM=N-1
   19 DO 2 J=2,MM
      IF (ALPHA(J).GE.1.0) GO TO 30
      IF (ALPHA(J).GE.A1P) GO TO 3
      A(J)=-2.
     C=ST1*TT*(1.-ALPHA(J)/A1P)
     C=ST3*TT*(2.+7.*PCPR)*((1.-A33(J))**.6666)*ACT
     C=ST4*TT*((1.-A44(J))**.6666)*ACT
      D(J)=0.
      GO TO 2
    3 IF(ALPHA(J) .GE. A2P) GOTO 5
      COTQ(J)=SQRT(COT(J))
      A(J)=-2.
     C=ST2*TT*SQRT(1.-(ALPHA(J)-A1P)/(A2P-A1P))*XX*COT(J)**(
     1                                                    XX-1.)
     C=ST3*TT*(2.+7.*PCPR)*((1.-A33(J))**.6666)*ACT
     C=ST4*TT*((1.-A44(J))**.6666)*ACT
      ZZ=1.- (ALPHA(J)-A1P)/(A2P-A1P)
      IF( ZZ .LE.  .00000000000000000001) ZZ=0.0
      D(J)=ST2*TT*(1.-XX)*(COT(J)**XX)*SQRT(ZZ)
      GO TO 2
    5 A(J)=-2.
     C=ST3*TT*(2.+7.*PCPR)*((1.-A33(J))**.6666)
     C=ST4*TT*((1.-A44(J))**.6666)
      D(J)=0.
      GO TO 2
   30 A(J)=-2.
      D(J)=0.
    2 CONTINUE
```

```
      DO 6 J=2,N
      Q(J-1)=B(J-1)/W(J-1)
      W(J)=A(J)-Z(J)*Q(J-1)
      G(J)=(D(J)-Z(J)*G(J-1))/W(J)
    6 CONTINUE
      CO(N)=G(N)
      DO 13 M=1,MM
      J=N-M
      CO(J)=G(J)-CO(J+1)*Q(J)
      IF (CO(J).LE.0.0) CO(J)=0.
   13 CONTINUE
      DO 14 J=1,MM
      IF( CO(J)  .LE. 0.000001) GOTO 14
      IF(ALPHA(J).LT.A1P)GOTO14
      IF(ALPHA(J) .GE. A2P) GO TO 14
      QQ=ABS((CO(J)-COT(J))/COT(J))
      IF (QQ.LE.0.08) GO TO 14
      GO TO 16
   14 CONTINUE
      GO TO 18
   16 DO 17 J=1,MM
      COT(J)=CO(J)
      IF (COT(J).LE.0.) COT(J)=0.00000000000000001*COB
   17 CONTINUE
      GO TO 19
   18 RETURN
      END
```

SUBROUTINE RATE

```
      SUBROUTINE RATE
      COMMON/JJJ/N,I,ALPRE,CO,DELT,ST1,ST2,ST3,PRE,COB,B,TT,
     CA1P,A2P,A2R,ALPHA,EST,Z,F,PRESP,RAVG,GRAD,TOTEXT,T,S1,
     CS2,L,S,K,PCPR,S4,S3,ST4,A44,A33,XX,ACT
      DIMENSION CO(250),ALPHA(250),B(250),Z(250),T(900),RAVG
     C(25),GRAD(25),TOTEXT(900),S(25),A44(250),A33(250)
      KF=INT(F)
      DO 1 J=1,N
      Q5=ALPHA(J)
      ACTB=EXP(-1.3734-7.5801*CO(J)**0.5+4.8712*CO(J))
      CQ=CO(J)/ACTB
      IF(CQ    .GT. 0.0050)GOTO48
      A44(J)=A44(J)+((1.-A44(J))**.6666)*(ST4*CO(J)*DELT/(
     C                                                .0050*S4))
      GOTO50
   48 A44(J)=A44(J)+((1.-A44(J))**.6666)*(ST4*DELT/S4)*ACT
   50 CONTINUE
      IF(CQ    .GT..010)GOTO20
      A33(J)=A33(J)+((1.-A33(J))**.6666)*(ST3*CO(J)*DELT/(0
     C                                                .010*S3))
      GOTO25
   20 A33(J)=A33(J)+((1.-A33(J))**.6666)*(ST3*DELT/S3)*ACT
   25 CONTINUE
      A1P=S1+A44(J)*S4+A33(J)*S3
      A2P=S1+S2+A44(J)*S4+A33(J)*S3
      IF(ALPHA(J) .GE. 1.0) GO TO 1
      IF(   (ALPHA(J)+A33(J)*S3+A44(J)*S4).GE. A1P) GOTO 2
      DADT=ST1*CO(J)*(1.-(ALPHA(J)/A1P))
      ALPHA(J)=ALPHA(J)+DELT*DADT+A33(J)*S3+A44(J)*S4
      IF((ABS(A1P-ALPHA(J))).LE. .01) ALPHA(J)=A1P
      IF(ALPHA(J) .LE. A1P) GO TO 1
      T7=DELT - (A1P-Q5)/DADT
      ALPHA(J)=A1P
      DADT=ST2*SQRT(1.-(ALPHA(J)-A1P)/(A2P-A1P))*(CO(J)**XX)
      ALPHA(J)=A1P+DADT*T7
      IF(ALPHA(J).GE.A2P)ALPHA(J)=A2P
      GOTO 1
    2 IF(   (ALPHA(J) + A44(J)*S4 + A33(J)*S3 ) .GE. A2P)
     C GOTO 3
      DADT=ST2*SQRT(1.-(ALPHA(J)-A1P)/(A2P-A1P))*(CO(J)**XX)
      ALPHA(J)=ALPHA(J)+DELT*DADT+A33(J)*S3+A44(J)*S4
      IF (ALPHA(J).GE.A2P) ALPHA(J)=A2P
      IF((A2P-ALPHA(J)).LE.0.01)ALPHA(J)=A2P
      GOTO 1
    3 ALPHA(J)=A2P
      IF (ALPHA(J).GE.0.99) ALPHA(J)=1.00
```

```
    1 CONTINUE
      DO 9 J=1,N
      IF (J.EQ.1) GO TO 9
      JQ=N+1-J
      IF(ALPHA(JQ) .GE. ALPHA(JQ+1))ALPHA(JQ)=ALPHA(JQ+1)
      IF (KF-1) 5,6,7
    5 ALPRE=ALPRE+(ALPHA(J)+ALPHA(J-1))/(2*(N-1))
      GO TO 8
    6 ALPRE=ALPRE+PRE*(J-1.5)*(ALPHA(J)+ALPHA(J-1))
      GO TO 8
    7 ALPRE=ALPRE+PRESP*(ALPHA(J)+ALPHA(J-1))*(7+J*(3*J-9))
    8 CONTINUE
      IF (ALPRE.GT.1.0) ALPRE=1.0
    9 CONTINUE
      RETURN
      END
```

☆U.S. GOVERNMENT PRINTING OFFICE: 1981-703-002/56 INT.-BU.OF MINES,PGH.,PA. 25396